ARTICLE

doi:10.1038/nature14893

The ubiquitin kinase PINK1 recruits autophagy receptors to induce mitophagy

Michael Lazarou[1]†*, Danielle A. Sliter[1]*, Lesley A. Kane[1]*, Shireen A. Sarraf[1], Chunxin Wang[1], Jonathon L. Burman[1], Dionisia P. Sideris[1], Adam I. Fogel[1] & Richard J. Youle[1]

Protein aggregates and damaged organelles are tagged with ubiquitin chains to trigger selective autophagy. To initiate mitophagy, the ubiquitin kinase PINK1 phosphorylates ubiquitin to activate the ubiquitin ligase parkin, which builds ubiquitin chains on mitochondrial outer membrane proteins, where they act to recruit autophagy receptors. Using genome editing to knockout five autophagy receptors in HeLa cells, here we show that two receptors previously linked to xenophagy, NDP52 and optineurin, are the primary receptors for PINK1- and parkin-mediated mitophagy. PINK1 recruits NDP52 and optineurin, but not p62, to mitochondria to activate mitophagy directly, independently of parkin. Once recruited to mitochondria, NDP52 and optineurin recruit the autophagy factors ULK1, DFCP1 and WIPI1 to focal spots proximal to mitochondria, revealing a function for these autophagy receptors upstream of LC3. This supports a new model in which PINK1–generated phospho–ubiquitin serves as the autophagy signal on mitochondria, and parkin then acts to amplify this signal. This work also suggests direct and broader roles for ubiquitin phosphorylation in other autophagy pathways.

Selective autophagy clears intracellular pathogens and mediates cellular quality control by engulfing cargo into autophagosomes and delivering it to lysosomes for degradation. Autophagy receptors bind ubiquitinated cargo and LC3-coated phagophores to mediate autophagy[1,2]. Damaged mitochondria are removed by autophagy after activation of the kinase PINK1 and the E3 ubiquitin ligase parkin (encoded by *PARK2* in humans)[3,4]. After the loss of mitochondrial membrane potential or the accumulation of misfolded proteins, PINK1 is stabilized on the outer mitochondrial membrane[3], where it phosphorylates ubiquitin at Ser65 to activate parkin ubiquitin ligase activity[5–7]. Although the autophagy receptors p62 and optineurin (OPTN) have been shown to bind ubiquitin chains on damaged mitochondria, their roles, and the roles of the other autophagy receptors in mediating mitophagy, are unclear[8–11].

Autophagy receptors in mitophagy

To clarify autophagy receptor function during mitophagy, genome editing was used to knock out five autophagy receptors (designated pentaKO) in HeLa cells, which do not express endogenous parkin. DNA sequencing (Supplementary Table 1) and immunoblotting of TAX1BP1, NDP52 (also known as CALCOCO2), NBR1, p62 (SQSTM1) and OPTN (Fig. 1a, lane 6) confirmed their knockout. We analysed mitophagy in pentaKOs by measuring the degradation of cytochrome C oxidase subunit II (COXII), a mitochondrial DNA (mtDNA)-encoded inner membrane protein, after mitochondrial damage with oligomycin and antimycin A. After oligomycin and antimycin A treatment, COXII was degraded in wild-type cells expressing parkin, but not in pentaKOs or ATG5 knockout HeLa cells, indicating a block in mitophagy (Fig. 1b, c, Supplementary Table 1 and Extended Data Fig. 1a). As a second indicator of mitophagy, mtDNA nucleoids were quantified by immunofluorescence (Extended Data Fig. 1b). After 24 h of oligomycin/antimycin A treatment, wild-type cells were nearly devoid of mtDNA, whereas mtDNA was retained in pentaKOs and ATG5 knockouts (Fig. 1d, e). Parkin translocated to mitochondria (Extended Data Fig. 1c), and MFN1 and TOM20 (also known as TOMM20) were degraded via the proteasome comparably in wild-type and pentaKOs (Fig. 1b and Extended Data Fig. 1d). mtDNA nucleoids clump after oligomycin and antimycin A treatment in ATG5 knockout cells, but not in pentaKOs, consistent with a reported role of p62 (refs 10, 11).

The five endogenous receptors in wild-type cells (Extended Data Fig. 1c) and each receptor re-expressed in pentaKOs (Extended Data Fig. 1e, f) translocated to mitochondria after oligomycin/antimycin A treatment. However, in pentaKOs, only green fluorescent protein (GFP)-tagged NDP52, GFP–OPTN and, to a lesser extent, GFP–TAX1BP1 rescued mitophagy (Fig. 1f, g). Another recently reported autophagy receptor, TOLLIP[12], neither recruited to mitochondria nor rescued mitophagy after oligomycin/antimycin A treatment (Extended Data Fig. 1g–i).

We generated OPTN and NDP52 single knockout, NDP52/OPTN double knockout (DKO), and NDP52/OPTN/TAX1BP1 triple knockout cell lines (Supplementary Table 1 and Fig. 1a), and found no compensatory change in the expression of the remaining receptors. NDP52 or OPTN knockout alone caused no defect in mitophagy, whereas the NDP52/OPTN DKO and to a greater extent the NDP52/OPTN/TAX1BP1 triple knockout inhibited mitophagy (Fig. 2a–d and Extended Data Fig. 2a, b). The robust mitophagy observed in OPTN knockouts contrasts with a report indicating loss of mitophagy using RNA interference (RNAi)-mediated knockdown of OPTN in HeLa cells[9]. Although NDP52 and OPTN redundantly mediate mitophagy, they function non-redundantly in xenophagy[13]. Their expression levels in human tissues indicate that OPTN or NDP52 may function more prominently in different tissues (Extended Data Fig. 2c).

Mutations in autophagy receptors can lead to diseases such as primary open angle glaucoma (OPTN; E50K)[14], amyotrophic lateral

[1]Biochemistry Section, Surgical Neurology Branch, National Institute of Neurological Disorders and Stroke, National Institutes of Health, Bethesda, Maryland 20892, USA. †Present address: Department of Biochemistry and Molecular Biology, Monash University, Clayton, Melbourne 3800, Australia.
*These authors contributed equally to this work.

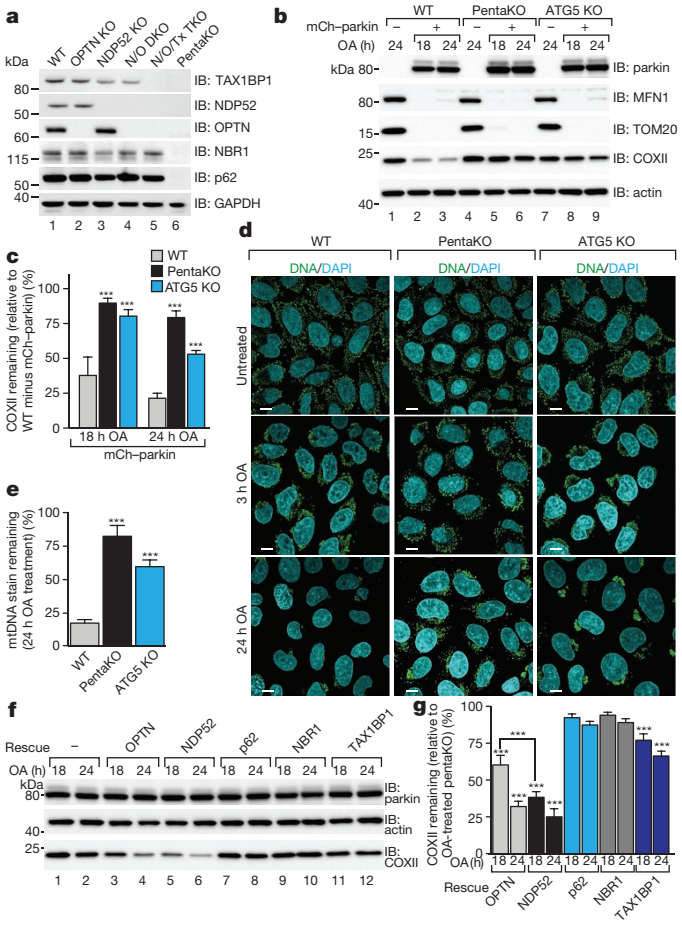

Figure 1 | Identifying autophagy receptors required for PINK1/parkin mitophagy. **a**, Wild-type (WT), OPTN knockout (KO), NDP52 knockout, NDP52/OPTN DKO (N/O DKO), NDP52/OPTN/TAX1BP1 triple knockout (N/O/Tx TKO), and pentaKO (NDP52/OPTN/TAX1BP1/NBR1/p62) HeLa cells were confirmed by immunoblotting (IB). kDa, kilodaltons. **b**, **c**, Cells as indicated with or without mCherry (mCh)–parkin were analysed by immunoblotting (**b**), and COXII levels were quantified (**c**). **d**, **e**, Representative images of mCh–parkin-expressing wild-type, pentaKO and ATG5 knockout cells immunostained to label mtDNA (green) (**d**), and quantified for mitophagy (24 h oligomycin/antimycin A (OA)) (**e**). More than 75 cells were counted per sample. DAPI, 4′,6-diamidino-2-phenylindole. Scale bars, 10 μm. **f**, **g**, Lysates from pentaKO cells expressing mCh–parkin and GFP-tagged autophagy receptors were immunoblotted (**f**) and COXII levels were quantified (**g**). Data in **c**, **e** and **g** are mean ± s.d. from three independent experiments. $^{***}P < 0.001$ (one-way analysis of variance (ANOVA)).

sclerosis (OPTN; E478G and Q398X, in which X denotes a stop codon)[15] and Crohn's disease (NDP52; V248A)[16]. Defects in xenophagy occur when OPTN is mutated to block its phosphorylation by TANK-binding kinase 1 (TBK1; S177A) or its ubiquitin binding (D474N)[13,17]. In pentaKOs, the UBAN domain-disrupting mutants OPTN (Q398X), OPTN(D474N) and OPTN(E478G) (Extended Data Fig. 2d) failed to translocate to mitochondria (Extended Data Fig. 2e, f) or rescue mitophagy (Fig. 2e and Extended Data Fig. 2g). OPTN(S177A) weakly rescued mitophagy and minimally translocated to mitochondria, whereas OPTN(E50K) robustly translocated and substantially rescued mitophagy (Fig. 2e and Extended Data Fig. 2e–g). NDP52(V248A) fully recruited to mitochondria and rescued mitophagy, but a mutant lacking the zinc-finger ubiquitin-binding domains (NDP52(ΔZF))[18] did not (Extended Data Fig. 2h–k and Fig. 2f). Thus, ubiquitin binding by OPTN and NDP52 is necessary for mitophagy, and some disease-causing mutations prevent mitophagy.

TBK1 and OPTN cooperate in mitophagy

TBK1 phosphorylation of OPTN at Ser177 increases its association with LC3 during xenophagy[13], and the OPTN(E50K) mutation increases TBK1 and OPTN binding[19]. TBK1 auto-phosphorylation at Ser172 is indicative of TBK1 activation[20] and occurs in a parkin-dependent manner after 3 h of oligomycin/antimycin A treatment, but only in cells expressing OPTN (Extended Data Fig. 3b, lanes 4 and 10). Prolonged oligomycin and antimycin A treatment induces moderate TBK1 phosphorylation in the absence of parkin, but still requires PINK1 (Extended Data Fig. 3c). To investigate TBK1 function during mitophagy, we generated TBK1 knockout, and TBK1/NDP52 and TBK1/OPTN DKO HeLa cells (Extended Data Fig. 3d and Supplementary Table 1). Parkin translocated to mitochondria in all cell lines, however, only TBK1/NDP52 DKOs displayed defective mitophagy (Extended Data Fig. 3e and Fig. 2g–j). Mitophagy in TBK1/NDP52 DKOs was rescued by wild-type TBK1 or phosphomimetic OPTN (OPTN(S177D)), but not by kinase-dead TBK1 (TBK1(K38M); Extended Data Fig. 3g–i). Thus, in the absence of NDP52, TBK1 is crucial for effective mitophagy via OPTN.

Ubiquitin phosphorylation in mitophagy

Although many autophagy receptors recruit to the mitochondria after parkin activation, it is unclear why only some of these function in mitophagy. Parkin-mediated mitophagy is driven by the PINK1 phosphorylation of Ser65 of both ubiquitin[5–7,21,22] and the parkin UBL domain[23]. Because Ser65 phospho-ubiquitin is structurally unique, it may differentially interact with ubiquitin-binding proteins[22]. To determine whether OPTN is directly recruited to phospho-ubiquitin on mitochondria, we conditionally expressed PINK1 on undamaged mitochondria[10] in HeLa cells lacking parkin (Fig. 3a and Extended Data Fig. 4a). When PINK1Δ110–YFP–2×FKBP (in which PINK1 lacks its N-terminal targeting sequence and is fused with yellow fluorescent protein (YFP) and two tandem FKBP domains at the C terminus) is cytosolic, mCherry-tagged OPTN (mCherry–OPTN), mCherry–NDP52 and mCherry–p62 are also cytosolic (Extended Data Fig. 4b, c). After rapalog treatment, PINK1Δ110–YFP–2×FKBP localizes to mitochondria expressing the FKBP12/rapamycin-binding (FRB)-Fis1 targeting construct where ubiquitin on mitochondrial surface proteins[24] (Extended Data Fig. 4a) can then be phosphorylated[5,21,25,26]. This recruits OPTN and NDP52 to mitochondria (Fig. 3a, b), but not p62 (Fig. 3b and Extended Data Fig. 4c). OPTN and NDP52 recruitment requires PINK1 kinase activity (Fig. 3a, b) and receptor–ubiquitin binding, as the OPTN(D474N) and NDP52(ΔZF) mutants fail to recruit after rapalog treatment (Fig. 3b and Extended Data Fig. 4d, e). Therefore, the ubiquitin kinase activity of PINK1 recruits OPTN and NDP52 to mitochondria via ubiquitin-binding domains in the absence of parkin.

To determine whether the observed autophagy receptor recruitment to mitochondria in the absence of parkin can induce mitophagy, we developed a sensitive fluorescence-activated cell sorting (FACS)-based mitophagy assay. We expressed mitochondrial-targeted mKeima (mt-mKeima, see Methods) in wild-type and pentaKO cells also expressing mitochondrial FRB-Fis1 and PINK1Δ110–YFP–2×FKBP. mt-mKeima engulfment into lysosomes results in a spectral shift owing to low pH. Only 1% (range 0.89–1.15) of wild-type or pentaKO cells display mitophagy when PINK1 is cytosolic. However, when PINK1 is recruited to mitochondria with rapalog, mitophagy increases ~sevenfold in wild-type cells and ~eightfold with overexpressed OPTN (Table 1 and Extended Data Fig. 5a). PentaKO cells showed no increase in mitophagy after targeting PINK1 to mitochondria (Table 1 and Extended Data Fig. 5b). When rescued with Flag/haemagglutinin (HA)-tagged OPTN or NDP52, pentaKOs displayed an increase in mitophagy of more than fivefold or fourfold, respectively (Table 1 and Extended Data Fig. 5b–e). Rescue with Flag/HA–p62 or ubiquitin-binding mutants (OPTN(Q398X), OPTN(D474N) and NDP52 (ΔZF)) failed to increase mitophagy above baseline, but

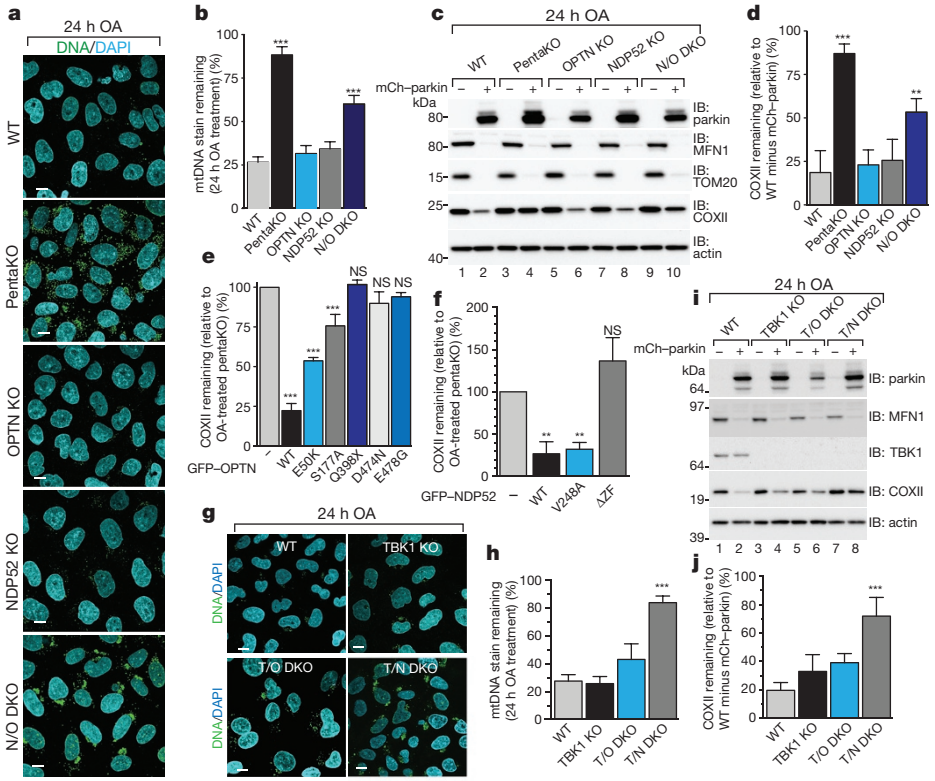

Figure 2 | OPTN and NDP52 are redundant in PINK1/parkin mitophagy. **a**, **b**, Representative images of wild-type, pentaKO, OPTN knockout, NDP52 knockout and NDP52/OPTN DKO cells expressing mCh–parkin immunostained with anti-DNA (green) (**a**), and quantified for mitophagy (**b**). **c**, **d**, Cell lines from **a** were analysed by immunoblotting (**c**), and COXII levels were quantified (**d**). **e**, COXII levels quantified from pentaKO cells expressing mCh–parkin and rescued with wild-type or mutant GFP–OPTN (see Extended Data Fig. 2g for blots). **f**, COXII levels quantified from pentaKOs expressing mCh–parkin rescued with wild-type or mutant GFP–NDP52 (see Extended Data Fig. 2k for blots). **g**, **h**, Representative images of wild-type, TBK1 knockout, TBK1/OPTN (T/O DKO) and TBK1/NDP52 (T/N DKO) HeLa cells expressing mCh–parkin and immunostained with anti-DNA (**g**), and quantification of mitophagy (**h**). **i**, **j**, Cells from **g** were immunoblotted (**i**) and COXII levels were quantified (**j**). Data in **b**, **d**–**f**, **h** and **i** are mean ± s.d. from three independent experiments. $^{**}P < 0.005$, $^{***}P < 0.001$ (one-way ANOVA). NS, not significant. More than 75 cells were measured per confocal sample. Scale bars, 10 μm. For untreated and mCh–parkin images of **a** and **g**, see Extended Data Fig. 3a and f, respectively.

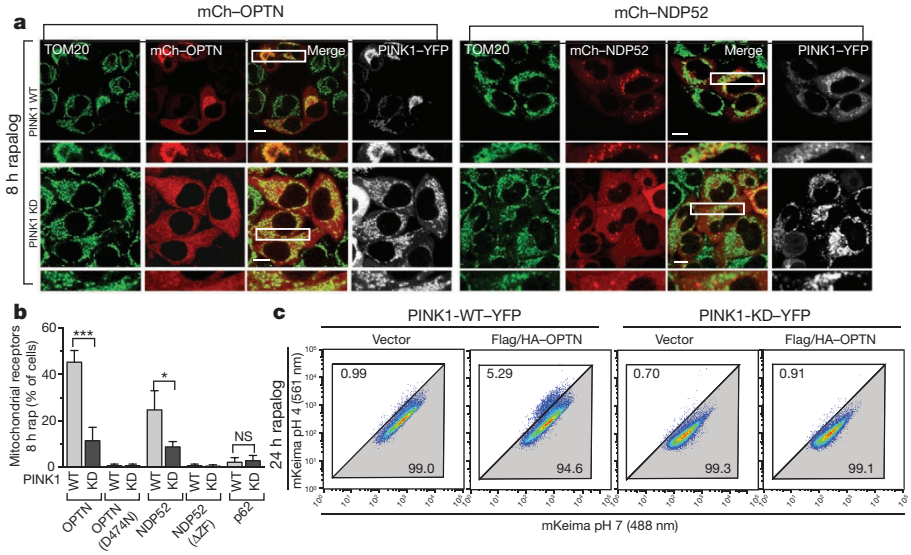

Figure 3 | PINK1 recruits OPTN and NDP52 independently of parkin to promote mitophagy. **a**, Representative images of HeLa cells expressing FRB-Fis1, wild-type or kinase-dead (KD) PINK1, PINK1Δ110–YFP–2×FKBP (PINK1–YFP), mCh–OPTN or mCh–NDP52, treated with rapalog. Scale bars, 10 μm. **b**, Quantification of receptor translocation in cells from **a** and Extended Data Fig. 4c–e. More than 100 cells were counted per sample. **c**, Cells were treated with rapalog and analysed by FACS for lysosomal-positive mt-mKeima. Representative data for wild-type or kinase-dead PINK1Δ110–YFP–2×FKBP in pentaKO cells with or without Flag/HA–OPTN expression. Data in **b** are mean ± s.d. from three independent experiments. $^{*}P < 0.05$, $^{***}P < 0.001$ (one-way ANOVA). For images of untreated cells from **a**, see Extended Data Fig. 4b.

Table 1 | Rapalog-induced mitophagy

Cell type	PINK1-YFP-2xFKBP	Receptor rescue	Receptor mutation	Parkin	Rap	Mean (%)	Fold change
WT	PINK1 WT	Vector	–	–	–	1.15	–
					+	8.37	7.28
		OPTN	WT	–	–	1.08	–
					+	8.59	7.95
PentaKO	PINK1 WT	Vector	–	–	–	0.93	–
					+	0.99	1.06
		OPTN	WT	–	–	0.89	–
					+	4.83	5.43
PentaKO	PINK1 WT	Vector	–	–	+	1.13	–
		OPTN	WT		+	5.27	4.66
	PINK1 KD	Vector	–	–	+	0.88	0.78
		OPTN	WT		+	0.76	0.67
PentaKO	PINK1 WT	Vector	–	–	+	0.93	–
		OPTN	WT		+	2.97	3.19
		OPTN	E50K		+	15.80	17.0
		OPTN	S177A		+	2.57	2.76
		OPTN	Q398X		+	0.87	0.78
		OPTN	D474N		+	0.76	0.67
	PINK1 WT	Vector	–	–	+	0.87	–
		NDP52	WT		+	3.50	3.98
		NDP52	V248A		+	2.80	3.18
		NDP52	ΔZF		+	0.47	0.53
		p62	WT		+	1.23	1.36
	PINK1 WT	OPTN	WT	–	–	1.10	–
		OPTN	WT		+	5.30	4.81
		OPTN	WT	+	–	1.43	–
		OPTN	WT		+	23.60	16.50

other mutants (OPTN(E50K), OPTN(S177A) and NDP52(V248A)) rescued mitophagy (Table 1 and Extended Data Fig. 5c–f). OPTN(E50K) and OPTN(S177A) restored mitophagy as well as or better than wild-type OPTN (Table 1), differing from their response in the presence of parkin (Fig. 2e), probably owing to the lack of robust TBK1 activation when parkin is absent (Extended Data Fig. 3b). Here, enhanced OPTN(E50K) binding to TBK1 (ref. 19) may become advantageous by allowing OPTN phosphorylation by TBK1 in the absence of parkin, thus improving mitophagy. In the absence of TBK1 activation, OPTN is probably not phosphorylated at Ser177 and thus is functionally similar to OPTN(S177A). Notably, the ubiquitin kinase activity of PINK1 is required, as kinase-dead PINK1 did not induce mitophagy (Table 1, Fig. 3c and Extended Data Fig. 5g). Parkin expression markedly increased mitophagy in Flag/HA–OPTN-expressing pentaKO cells (Table 1 and Extended Data Fig. 5h), supporting the model that PINK1-phosphorylated ubiquitin recruits receptors for mitophagy, and parkin ubiquitination of mitochondrial substrates amplifies this signal.

Comparing mitophagy induced by oligomycin/antimycin A treatment in wild-type relative to PINK1 knockout cells confirmed that endogenous PINK1 mediates mitophagy in the absence of parkin (Extended Data Fig. 6a, b). Re-expressing PINK1 in PINK1-knockout cells rescued oligomycin/antimycin-A-induced mitophagy (Extended Data Fig. 6c, d). Furthermore, mCherry–OPTN is recruited to mitochondria in the absence of parkin in a PINK1-dependent manner after prolonged exposure to oligomycin/antimycin A (Extended Data Fig. 6e, f).

Given that PINK1 ubiquitin kinase activity can recruit OPTN and NDP52, we investigated autophagy receptor binding to phosphomimetic (S65D) HA–ubiquitin in HeLa cells. Endogenous OPTN and NDP52 preferentially co-immunoprecipitate with HA–ubiquitin(S65D) (Extended Data Fig. 7a). Conversely, p62 was present at equal levels in all co-immunoprecipitates (Extended Data Fig. 7a). Ubiquitin-modified and unmodified forms of OPTN and NDP52 were present in co-immunoprecipitates, and HA–ubiquitin(S65D) induced or preserved this modification (Extended Data Fig. 7a). Co-immunoprecipitated samples treated with the deubiquitinase USP2 removed the ubiquitin-modified bands on OPTN and NDP52, yet OPTN and NDP52 retained HA–ubiquitin(S65D) binding (Extended Data Fig. 7b). The binding of endogenous receptors in HeLa cell cytosol to *in vitro* phosphorylated strep-tactin-tagged ubiquitin (Extended Data Fig. 7c) showed that OPTN, but not p62, bound better to phospho-ubiquitin (Extended Data Fig. 7d, e). However, recombinant glutathione *S*-transferase (GST)–OPTN did not bind better to *in vitro* phosphorylated Lys63-linked ubiquitin chains[27], indicating that OPTN may need additional factors or modification *in vivo* to bind Ser65-phosphorylated ubiquitin preferentially.

OPTN and NDP52 recruit upstream machinery

Autophagy receptors are thought to function primarily by bridging LC3 and ubiquitinated cargo[1,2]. In mCherry–parkin wild-type cells, GFP–LC3B accumulated in distinct puncta adjacent to mitochondria after oligomycin/antimycin A treatment (Extended Data Fig. 8a). Although oligomycin and antimycin A also induced GFP–LC3B puncta in pentaKOs, they were fewer and not near mitochondria (Extended Data Fig. 8a). Conversely, GFP–LC3B in ATG5 knockouts was near mitochondria, but not in puncta (Extended Data Fig. 8a). LC3B lipidation is retained in pentaKOs, but lost in ATG5 knockouts (Extended Data Fig. 8b). This indicates that ATG5 is activated downstream of PINK1, but independently of autophagy receptors, and that LC3 mitochondrial localization and lipidation are independent steps of mitophagy.

OPTN and NDP52 interact with LC3B and LC3C, respectively, for *Salmonella* clearance[13,28]. Beyond that, little is known about the specificity of LC3 family members towards autophagy receptors[29] or their involvement in mitophagy. We examined the recruitment of all LC3 and GABARAP family members to mitochondria in wild-type, pentaKO and NDP52/OPTN DKO cells. The oligomycin/antimycin-A-induced mitochondrial localization of GFP–LC3s in wild-type cells was absent in pentaKO cells, while only GFP–LC3B recruitment was inhibited in NDP52/OPTN DKOs (Fig. 4a and Extended

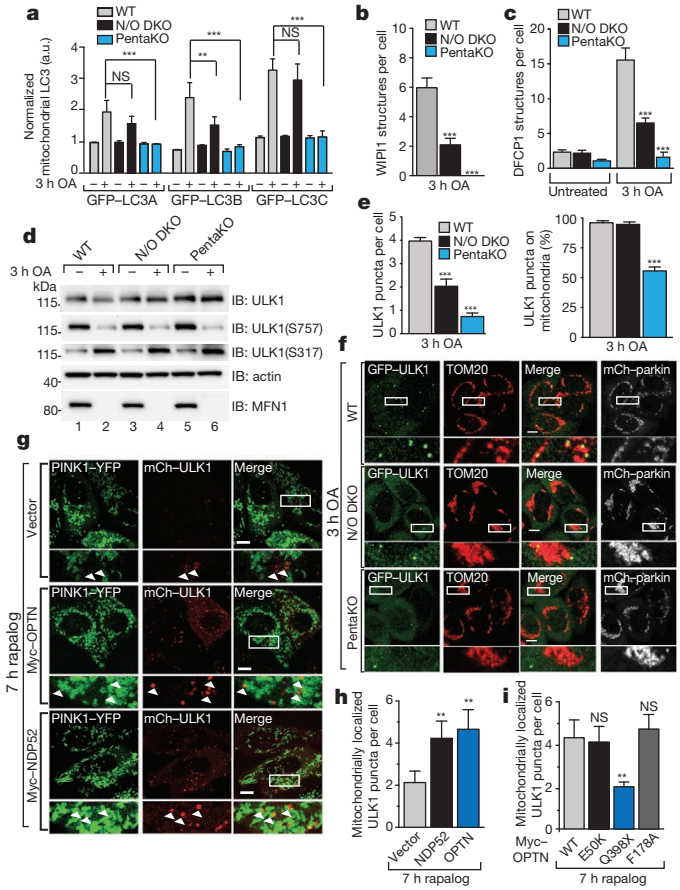

Figure 4 | Characterization of autophagy receptor function during mitophagy. a–d, mCh–parkin-expressing wild-type, NDP52/OPTN DKO and pentaKO cells were quantified for GFP–LC3A, GFP–LC3B and GFP–LC3C translocation to mitochondria (**a**), and for GFP–WIPI1 (**b**) or GFP–DFCP1 (**c**) structures per cell (>100 cells counted for each sample), or were immunoblotted using phospho-specific anti-S757 and anti-S317 ULK1 antibodies (**d**). **e**, mCh–parkin wild-type, NDP52/OPTN DKO and pentaKO cells stably expressing GFP–ULK1 were quantified for GFP–ULK1 puncta per cell (left), and the percentage of those puncta on mitochondria was determined (right). **f**, Representative cells from **e** were immunostained for TOM20 and GFP. **g**, PentaKO cells expressing FRB-Fis1, PINK1Δ110–YFP–2×FKBP, mCh–ULK1 and Myc-tagged receptors were treated with rapalog and then imaged live. **h**, Quantification of mitochondrial ULK1 puncta in **g**. **i**, Quantification of mitochondrial ULK1 puncta in pentaKO cells expressing FRB-Fis1, PINK1Δ110–YFP–2×FKBP, mCh–ULK1 and Myc–OPTN mutants, treated with rapalog then imaged live. Data in **a–c**, **e**, **h** and **i** are mean ± s.d. from three independent experiments. $^{**}P < 0.005$, $^{***}P < 0.001$ (one-way ANOVA). For live-cell quantification, >75 cells were counted in a blinded manner. Quantifications in **h** and **i** were performed after removal of outliers; see Methods for details. Scale bars, 10 μm. a.u., arbitrary units. See Extended Data Figs 8c, 9b, c and 10d for representative images of **a**, **b**, **c** and **i**, respectively. See Extended Data Fig. 9e for untreated samples of **f**, and Extended Data Fig. 10c for untreated images of **h** and **i**.

Data Fig. 8c). GFP–LC3C recruitment was inhibited in NDP52/OPTN/TAX1BP1 triple knockouts (Extended Data Fig. 8d, e), indicating that TAX1BP1 can recruit LC3C during mitophagy. GABARAP proteins did not recruit to mitochondria, indicating that they probably do not have a substantial role in mitophagy (Extended Data Fig. 9a).

We also examined the involvement of WIPI1 and DFCP1, two proteins that mediate phagophore biogenesis upstream of LC3 (ref. 30), in mitophagy. In wild-type cells, oligomycin/antimycinA-induced foci of both GFP–WIPI1 and GFP–DFCP1, mostly localized on or near mitochondria (Fig. 4b, c and Extended Data Fig. 9b, c). In NDP52/OPTN DKO cells, GFP–WIPI1 and GFP–DFCP1 foci were reduced, and almost undetectable in pentaKO cells (Fig. 4b, c and Extended Data Fig. 9b, c). Despite this, the phosphorylation of beclin1 (ref. 31) was normal in both pentaKO and NDP52/OPTN DKO cells (Extended Data Fig. 9d), indicating that failure to recruit WIPI1 and DFPC1 was not due to a defective VPS34 (also known as PIK3C3) complex. GFP–DFCP1 recruitment in pentaKO cells was rescued by the expression of Flag/HA–OPTN or Flag/HA–NDP52, but not by Flag/HA–p62 (Extended Data Fig. 10a).

Although autophagy receptors are thought to function late in autophagy with LC3 (ref. 32), the deficit in WIPI1 and DFCP1 recruitment to mitochondria indicates a defect upstream in autophagosome biogenesis. ULK1 phosphorylation by AMPK at Ser317 and dephosphorylation at Ser757 (ref. 33), required for activation, occurs comparably in wild-type, NDP52/OPTN DKO and pentaKO cells (Fig. 4d). Despite this, ULK1 puncta appearance[34] after oligomycin and antimycin A treatment is diminished by half in the NDP52/OPTN DKO cells, and by more than 80% in pentaKO cells (Fig. 4e, f). Flag/HA–OPTN or Flag/HA–NDP52, but not Flag/HA–p62, rescued GFP–ULK1 localization in pentaKO cells (Extended Data Fig. 10b). Overall, these data indicate that NDP52 and OPTN recruit ULK1 to initiate mitophagy.

We next assessed whether ubiquitin phosphorylation, independent of parkin, is also sufficient to recruit ULK1 to mitochondria. Rescue of pentaKO cells expressing FRB-Fis1 and PINK1Δ110–YFP–2×FKBP with Myc–OPTN or Myc–NDP52 resulted in mitochondrial ULK1 puncta after rapalog treatment (Fig. 4g, h). Myc–OPTN(E50K) also rescued ULK1 recruitment to mitochondria, but mutant Myc–OPTN(Q398X), which is associated with amyotrophic lateral sclerosis, did not (Fig. 4i and Extended Data Fig. 10d). ULK1 recruitment was restored by Myc–OPTN(F178A) (Fig. 4i and Extended Data Fig. 10d), a mutation that disrupts OPTN association with LC3 (ref. 13), indicating that ULK1 recruitment is not through LC3 interaction and occurs upstream of LC3 (ref. 34). Taken together, our data show that PINK1 ubiquitin kinase activity is sufficient to recruit the autophagy receptors and upstream autophagy machinery to mitochondria to induce mitophagy.

Conclusions

Through the genetic knockout of five autophagy receptors, we have defined their relative roles in mitophagy and identified their unanticipated upstream involvement in autophagy recruitment machinery. p62 and NBR1 are dispensable for parkin-mediated mitophagy; OPTN and NDP52 are the primary, yet redundant, receptors. We also uncovered a new and more fundamental role for PINK1 in mitophagy: to induce mitophagy directly through phospho-ubiquitin-mediated recruitment of autophagy receptors. We propose that PINK1 generates the novel and essential signature (phospho-ubiquitin) on mitochondria to induce OPTN and NDP52 recruitment and mitophagy; parkin acts to increase this signal by generating more ubiquitin chains on mitochondria, which are subsequently phosphorylated by PINK1. Our findings clarify the role of parkin as an amplifier of the PINK1-generated mitophagy signal, phospho-ubiquitin, which can engage the autophagy receptors to recruit ULK1, DFCP1, WIPI1 and LC3 (see model in Extended Data Fig. 10e).

Online Content Methods, along with any additional Extended Data display items and Source Data, are available in the online version of the paper; references unique to these sections appear only in the online paper.

Received 8 January; accepted 10 July 2015.
Published online 12 August 2015.

1. Svenning, S. & Johansen, T. Selective autophagy. *Essays Biochem.* **55,** 79–92 (2013).
2. Stolz, A., Ernst, A. & Dikic, I. Cargo recognition and trafficking in selective autophagy. *Nature Cell Biol.* **16,** 495–501 (2014).
3. Narendra, D. P. *et al.* PINK1 is selectively stabilized on impaired mitochondria to activate parkin. *PLoS Biol.* **8,** e1000298 (2010).

4. Narendra, D., Tanaka, A., Suen, D. F. & Youle, R. J. Parkin is recruited selectively to impaired mitochondria and promotes their autophagy. *J. Cell Biol.* **183,** 795–803 (2008).
5. Kane, L. A. *et al.* PINK1 phosphorylates ubiquitin to activate Parkin E3 ubiquitin ligase activity. *J. Cell Biol.* **205,** 143–153 (2014).
6. Kazlauskaite, A. *et al.* Parkin is activated by PINK1-dependent phosphorylation of ubiquitin at Ser65. *Biochem. J.* **460,** 127–139 (2014).
7. Koyano, F. *et al.* Ubiquitin is phosphorylated by PINK1 to activate parkin. *Nature* **510,** 162–166 (2014).
8. Geisler, S. *et al.* PINK1/Parkin-mediated mitophagy is dependent on VDAC1 and p62/SQSTM1. *Nature Cell Biol.* **12,** 119–131 (2010).
9. Wong, Y. C. & Holzbaur, E. L. F. Optineurin is an autophagy receptor for damaged mitochondria in parkin-mediated mitophagy that is disrupted by an ALS-linked mutation. *Proc. Natl Acad. Sci. USA* **111,** E4439–E4448 (2014).
10. Narendra, D., Kane, L. A., Hauser, D. N., Fearnley, I. M. & Youle, R. J. p62/SQSTM1 is required for Parkin-induced mitochondrial clustering but not mitophagy; VDAC1 is dispensable for both. *Autophagy* **6,** 1090–1106 (2010).
11. Okatsu, K. *et al.* p62/SQSTM1 cooperates with Parkin for perinuclear clustering of depolarized mitochondria. *Genes Cells* **15,** 887–900 (2010).
12. Lu, K., Psakhye, I. & Jentsch, S. Autophagic clearance of polyQ proteins mediated by ubiquitin-Atg8 adaptors of the conserved CUET protein family. *Cell* **158,** 549–563 (2014).
13. Wild, P. *et al.* Phosphorylation of the autophagy receptor optineurin restricts Salmonella growth. *Science* **333,** 228–233 (2011).
14. Rezaie, T. *et al.* Adult-onset primary open-angle glaucoma caused by mutations in optineurin. *Science* **295,** 1077–1079 (2002).
15. Maruyama, H. *et al.* Mutations of optineurin in amyotrophic lateral sclerosis. *Nature* **465,** 223–226 (2010).
16. Ellinghaus, D. *et al.* Association between variants of PRDM1 and NDP52 and Crohn's disease, based on exome sequencing and functional studies. *Gastroenterology* **145,** 339–347 (2013).
17. Mankouri, J. *et al.* Optineurin negatively regulates the induction of IFNβ in response to RNA virus infection. *PLoS Pathog.* **6,** e1000778 (2010).
18. Thurston, T. L., Ryzhakov, G., Bloor, S., von Muhlinen, N. & Randow, F. The TBK1 adaptor and autophagy receptor NDP52 restricts the proliferation of ubiquitin-coated bacteria. *Nature Immunol.* **10,** 1215–1221 (2009).
19. Morton, S., Hesson, L., Peggie, M. & Cohen, P. Enhanced binding of TBK1 by an optineurin mutant that causes a familial form of primary open angle glaucoma. *FEBS Lett.* **582,** 997–1002 (2008).
20. Larabi, A. *et al.* Crystal structure and mechanism of activation of TANK-binding kinase 1. *Cell Rep.* **3,** 734–746 (2013).
21. Ordureau, A. *et al.* Quantitative proteomics reveal a feedforward mechanism for mitochondrial PARKIN translocation and ubiquitin chain synthesis. *Mol. Cell* **56,** 360–375 (2014).
22. Wauer, T. *et al.* Ubiquitin Ser65 phosphorylation affects ubiquitin structure, chain assembly and hydrolysis. *EMBO J.* **34,** 307–325 (2015).
23. Kondapalli, C. *et al.* PINK1 is activated by mitochondrial membrane potential depolarization and stimulates Parkin E3 ligase activity by phosphorylating Serine 65. *Open Biol.* **2,** 120080 (2012).
24. Sarraf, S. A. *et al.* Landscape of the PARKIN-dependent ubiquitylome in response to mitochondrial depolarization. *Nature* **496,** 372–376 (2013).
25. Shiba-Fukushima, K. *et al.* Phosphorylation of mitochondrial polyubiquitin by PINK1 promotes Parkin mitochondrial tethering. *PLoS Genet.* **10,** e1004861 (2014).
26. Okatsu, K. *et al.* Phosphorylated ubiquitin chain is the genuine Parkin receptor. *J. Cell Biol.* **209,** 111–128 (2015).
27. Ordureau, A. *et al.* Defining roles of PARKIN and ubiquitin phosphorylation by PINK1 in mitochondrial quality control using a ubiquitin replacement strategy. *Proc. Natl Acad. Sci. USA* **112,** 6637–6642 (2015).
28. von Muhlinen, N. *et al.* LC3C, bound selectively by a noncanonical LIR motif in NDP52, is required for antibacterial autophagy. *Mol. Cell* **48,** 329–342 (2012).
29. Wild, P., McEwan, D. G. & Dikic, I. The LC3 interactome at a glance. *J. Cell Sci.* **127,** 3–9 (2014).
30. Lamb, C. A., Yoshimori, T. & Tooze, S. A. The autophagosome: origins unknown, biogenesis complex. *Nature Rev. Mol. Cell Biol.* **14,** 759–774 (2013).
31. Fogel, A. I. *et al.* Role of membrane association and Atg14-dependent phosphorylation in beclin-1-mediated autophagy. *Mol. Cell. Biol.* **33,** 3675–3688 (2013).
32. Koyama-Honda, I., Itakura, E., Fujiwara, T. K. & Mizushima, N. Temporal analysis of recruitment of mammalian ATG proteins to the autophagosome formation site. *Autophagy* **9,** 1491–1499 (2013).
33. Kim, J., Kundu, M., Viollet, B. & Guan, K. L. AMPK and mTOR regulate autophagy through direct phosphorylation of Ulk1. *Nature Cell Biol.* **13,** 132–141 (2011).
34. Itakura, E., Kishi-Itakura, C., Koyama-Honda, I. & Mizushima, N. Structures containing Atg9A and the ULK1 complex independently target depolarized mitochondria at initial stages of Parkin-mediated mitophagy. *J. Cell Sci.* **125,** 1488–1499 (2012).

Supplementary Information is available in the online version of the paper.

Acknowledgements We thank C. Nezich and S. Banerjee in the Youle laboratory, C. Smith and the NINDS and NHLBI Flow Cytometry Core Facilities. This work was supported by the Intramural Research Program of the NIH, NINDS and the National Health and Medical Research Council (GNT1063781).

Author Contributions M.L., D.A.S., L.A.K. and R.J.Y. conceived the projects; M.L., D.A.S., L.A.K., S.A.S., C.W., D.P.S., A.I.F. and R.J.Y. designed experiments; M.L., D.A.S., L.A.K., S.A.S., C.W., J.L.B., D.P.S. and A.I.F. performed experiments; M.L., D.A.S., L.A.K. and R.J.Y. wrote the manuscript, and all authors contributed to editing the manuscript.

Author Information Reprints and permissions information is available at www.nature.com/reprints. The authors declare no competing financial interests. Readers are welcome to comment on the online version of the paper. Correspondence and requests for materials should be addressed to R.J.Y. (youler@ninds.nih.gov).

METHODS

Cell culture, antibodies and reagents. HEK293T, HeLa and PINK1 knockout cells[35] were cultured in DMEM (Life Technologies) supplemented with 10% (v/v) FBS (Gemini Bio Products), 10 mM HEPES (Life Technologies), 1 mM sodium pyruvate (Life Technologies), non-essential amino acids (Life Technologies) and GlutaMAX (Life Technologies). HeLa cells were acquired from the ATCC and authenticated by the Johns Hopkins GRCF Fragment Analysis Facility using STR profiling. All cells were tested for mycoplasma contamination bimonthly using the PlasmoTest kit (InvivoGen). Transfection reagents used were: effectene (Qiagen), lipofectamine LTX (Life Technologies), avalanche-OMNI (EZ Biosystems), X-tremeGENE HP (Roche) and X-tremeGENE 9 (Roche).

The following rabbit monoclonal and polyclonal antibodies were used: beclin, pULK1(S317), pULK1(S757), TBK1, pTBK1(S172), NDP52, TAX1BP1, ATG5, actin, and haemagglutinin (Cell Signaling Technologies); GAPDH and LC3B (Sigma); ULK1 and TOM20 (Santa Cruz Biotechnology); OPTN (Proteintech); GFP (Life Technologies); pSer65 ubiquitin (Millipore) and MFN1 was generated previously[36]. Mouse monoclonal antibodies used were: NBR1 and p62 (Abnova), COXII (Abcam), parkin (Santa Cruz Biotechnology), DNA (Progen Biotechnik) and ubiquitin (Cell Signaling). Chicken anti-GFP (Life Technologies) was also used. For catalogue numbers, see Supplementary Table 1. Human tissue panel blots were purchased (NOVUS Biologicals).

Generation of knockout lines using TALEN and CRISPR/Cas9 gene editing. To generate knockout cell lines, transcription activator-like effector nuclease (TALEN) and CRISPR guide RNAs (gRNAs) were chosen that targeted an exon common to all splicing variants of the gene of interest (listed in Supplementary Table 1). TALEN was used to generate the OPTN knockout HeLa cell line. The TALEN constructs were generated by sequential ligation of coding repeats into pcDNA3.1/Zeo-Talen(+63), as previously described[37–39]. The CRISPR/Cas9 system generated previously[40] was used to knockout ATG5, NDP52, TAX1BP1, NBR1, p62 and TBK1. Oligonucleotides (Operon) containing CRISPR target sequences were annealed and ligated into AlfII-linearized gRNA vector (Addgene 41824)[40]. For CRISPR/Cas9 gene editing, HeLa cells were transfected with gRNA constructs, hCAS9 (Addgene 41815) and pEGFP-C1 (Clontech). For TALEN gene editing, HeLa cells were transfected with OPTN TALEN constructs and pEGFP-C1. Two days after transfection, GFP-positive cells were sorted by FACS and plated in 96-well plates. Single colonies were expanded into 24-well plates before screening for depletion of the targeted gene product by immunoblotting. As a secondary screen of some knockout lines, genomic DNA was isolated from cells and the genomic regions of interest were amplified using PCR followed restriction enzyme digestion analysis (primers listed in Supplementary Table 1). Sequencing of targeted genomic regions of knockout lines was also conducted to confirm the presence of frameshifting indels in the genes of interest (Supplementary Table 1). To generate multiple gene knockout cell lines, parental cell lines were transfected sequentially with one or multiple gRNA constructs to generate desired knockout lines. Parental cell lines are outlined in Supplementary Table 1.

Cloning and generation of stable cell lines. pMXs-puro-GFP-WIPI1 and pMXs-puro-GFP-DFCP1 were a gift from N. Mizushima, and pMXs-IP-GFP-ULK1 was purchased from Addgene (38193). To generate pBMN-mEGFP-C1, mEGFP-C1 (Addgene 36412) was PCR amplified (together with the multiple cloning site) and cloned into pBMN-Z at BamHI/SalI sites using the Gibson Cloning kit (New England BioLabs) according to the manufacturer's instructions. The BamHI and SalI sites used to insert mEGFP-C1 were not regenerated. The following GFP-tagged plasmids were generated by PCR amplification of open reading frames followed by ligation into pBMN-mEGFP-C1: OPTN, NDP52, p62, TAX1BP1, NBR1, LC3A, LC3B, LC3C, GABARAP, GABARAPL1 and GABARAPL2. The Gateway Cloning (Invitrogen) system was used to generate GFP-, mCherry-, Myc- and Flag/HA-tagged constructs. In brief, TBK1, TBK1(K38M), NDP52, OPTN, p62, DFCP1, WIPI1 and ULK1 were cloned into pDONR2333. Mutations in complementary DNA sequences were introduced using PCR site-directed mutagenesis in the pDONR2333 vector, (sequences of mutagenesis primers used are available on request) then recombined into pHAGE-N-Flag/HA, pHAGE-N-GFP, pHAGE-N-mCherry and/or pDEST-N-myc using LR Clonase (Invitrogen) as per the manufacturer's protocol. All constructs generated in this study were verified by sequencing.

To generate stably transfected cell lines, retroviruses (for pBMN-mEGFP-C1 constructs, pBMN-mCherry-parkin, pBMN-puro-P2A-FRB-Fis1, pCHAC-mt-mKeima-IRES-MCS2) and lentiviruses (for pHAGE and pDEST constructs) were packaged in HEK293T cells. HeLa cells were transduced with virus for 24 h with 8 $\mu g\,ml^{-1}$ polybrene (Sigma) then optimized for protein expression via selection (puromycin or blasticidin) or fluorescence sorting.

Translocation and mitophagy treatments. Cells were either left untreated or treated with 10 μM oligomycin (Calbiochem), 4 μM antimycin A (Sigma) in fresh growth medium for different periods of time as indicated. Some experiments were performed with 10 μM carbonyl cyanide *m*-chlorophenyl hydrazine (CCCP) as indicated (Sigma-Aldrich). We chose to use oligomycin/antimycin A to depolarize mitochondria in most of our experiments, as they are specific mitochondrial respiratory complex inhibitors and less toxic. Long treatment time points of both oligomycin/antimycin A and CCCP were also supplemented with the apoptosis inhibitor 20 μM QVD (ApexBio) to prevent cell death.

Immunoblotting and phos-tag gels. HeLa cells seeded into six-well plates were either untreated or treated with 10 μM oligomycin (Calbiochem), 4 μM antimycin A (Sigma) and 20 μM QVD (ApexBio) in fresh growth medium for different periods of time as indicated. Cells were lysed in 1× LDS sample buffer (Life Technologies) supplemented with 100 mM dithiothreitol (DTT; Sigma) and heated to 99 °C with shaking for 7–10 min. Approximately 25–50 μg of protein per sample was separated on 4–12% Bis-Tris gels (Life Technologies) according to manufacturer's instructions, and then transferred to polyvinyl difluoride membranes and immunoblotted using antibodies as indicated. To assess mitophagy, COXII quantification was conducted using ImageLab software (BioRad). For uncropped images of all immunoblots, see Supplementary Information.

To dephosphorylate samples, cells were collected as above and lysed in 1× NEB buffer 3 (New England BioLabs) supplemented with 1% Triton X-100 and passed through a 26.5-gauge needle. Calf intestinal phosphatase (CIP; New England BioLabs) was added to half of the cell lysate and the other half was used as an untreated control. Both samples were incubated for 1 h at 37 °C and analysed by SDS–PAGE and immunoblotting.

To analyse beclin phosphorylation, lysates were prepared in sample buffer lacking EDTA and run on 8% Tris-glycine gels containing 20 μM phos-tag (Wako) and 40 μM $MnCl_2$ as described previously[31]. Gels lacking phos-tag were run simultaneously as a negative control. Electrophoresis and western transfer were carried out using standard protocols with the exception that phos-tag gels were incubated in 10 mM EDTA for 10 min to remove excess Mn^{2+} before transfer.

Immunoprecipitation. Wild-type or PINK1 knockout HeLa cells were transiently transfected with HA-tagged ubiquitin, ubiquitin(S65A) or ubiquitin(S65D) with or without mCherry–parkin for 24 h. Cells were collected, lysed and the HA–ubiquitin was immunoprecipitated as reported previously[5], using anti-HA-conjugated beads (Pierce). To deubiquitinate the bound proteins, after binding the HA–ubiquitin, beads were washed three times and incubated in 50 mM Tris-HCl, pH 7.5, 150 mM NaCl, 5 mM DTT and 1.47 μg USP2 (Boston Biochem) at 37 °C for 1 h. The reaction was stopped and the remaining bound proteins were washed five times with 1 ml of buffer (50 mM Tris-HCl, pH 7.5, 150 mM NaCl), and then eluted by boiling with 1× LDS sample buffer.

***In vitro* phosphorylation.** Strep-tagged ubiquitin was incubated with either wild-type or kinase-dead *Tribolium castaneum* PINK1 (TcPINK1) as previously reported[5]. This ubiquitin was then incubated with cytosol from wild-type HeLa cells in 20 mM HEPES-KOH, pH 7.6, 220 mM mannitol and 70 mM sucrose at 4 °C for 1 h. Strep-tactin beads (Qiagen) were then added to bind the strep–ubiquitin for an additional 1 h at 4 °C. The ubiquitin and bound proteins were then eluted with 50 mM biotin in 50 mM Tris for 15 min at room temperature. Samples were then diluted in LDS sample buffer before SDS–PAGE and immunoblot analysis.

Immunofluorescence microscopy. HeLa cells, seeded in two-well chamber slides (Lab-Tek), were treated as indicated in the figure legends. After treatment, cells were rinsed in PBS and fixed for 15 min at room temperature with 4% paraformaldehyde. Cells were then permeabilized and blocked with 0.1% Triton X-100, 3% goat serum in PBS for 40 min. For immunostaining, cells were incubated with antibodies (as indicated in figure legends) diluted in 3% goat blocking serum overnight at 4 °C, then rinsed with PBS and incubated with either anti-rabbit or mouse Alexa-Fluor-488- and Alexa-Fluor-633-conjugated secondary antibodies (Life Technologies), or anti-chicken Alexa-Fluor-488-conjugated antibody (Life Technologies) for 1 h at room temperature. Cells were washed three times for 5 min each with 1% Triton X-100 in PBS. During the final wash step, cells were incubated with 10 $\mu g\,ml^{-1}$ DAPI (Sigma) in PBS for 5 min. To measure mitophagy by mtDNA immunostaining, images were obtained from samples stained with DAPI and immunostained for DNA using a plan-Apochromat 63×/1.4 oil DIC objective on an LSM 510 microscope (Zeiss). Four image slices were collected through the *Z* plane encompassing the top and bottom of the cells. Image analysis was performed on all images collected in the *Z* plane using Volocity software (Perkin Elmer v6.0.1). The percentage of mtDNA stain remaining was calculated using the following formula: $(cDNA_v - nDNA_v)/n$, in which $cDNA_v$ is the total cellular DNA volume determined by staining using anti-DNA antibodies, and $nDNA_v$ is the total nuclear DNA stain volume determined using DAPI, and n denotes the number of cells.

The mtDNA stain volume in untreated cells was normalized to 100% and the amount of mtDNA stain remaining after drug treatment was subsequently determined. Final values represent data acquired from 50–200 cells from three independent experiments, and investigators were not blinded to allocation during image analysis.

To analyse LC3/mitochondrial protein colocalization; cells were treated, fixed and immunostained as above. Between 5 and 8 slices were imaged through the *Z* plane using either a plan-Apochromat 63× or 100×/1.4 oil DIC objective on a CW STED confocal microscope (Leica). Volocity software (Perkin Elmer, v6.0.1) was used to measure the intensity of the GFP signal representing LC3 in the volume occupied by mitochondria (as defined by the TOM20-positive region) and the cytosol (as defined by TOM20-negative region). 'Normalized mitochondrial LC3' was calculated using the following formula: normalized mitochondrial LC3 = $(m_i/m_v)/(c_i/c_v)$, in which m_i denotes the mitochondrial GFP intensity, m_v denotes the mitochondrial volume, c_i denotes the cytosolic GFP intensity, and c_v denotes the cytosolic volume. The resulting normalized mitochondrial LC3 is equal to 1 if the intensity of GFP is equal per volume in the cytosolic and mitochondrial volumes (no translocation) and is above one if the mitochondrial intensity is higher per volume (translocation). Final values for normalized mitochondrial LC3 represents data acquired from 50 to 105 cells from three independent experiments.

For GFP–DFCP1, GFP–WIPI1 and GFP–ULK1 puncta analysis, cells were treated, prepared and imaged on the CW STED as above with the addition of immunostaining using either rabbit or chicken GFP antibodies to enhance the signal in the green channel. GFP–DFCP1 puncta were quantified using Volocity software (Perkin Elmer v6.0.1) and GFP–WIPI1 and GFP–ULK1 puncta were quantified manually. Investigators were not blinded to allocation during image analysis. Colocalization of autophagy receptors with GFP–DFCP1 or GFP–ULK1 was assessed with line scans using LAS AF software (Leica, v.2.6.0.7266).

Heterodimerization. The C-terminal Fis1 tail of human Fis1 (amino acids 92–152) was cloned into pC4-RhE vector (ARIAD) at SpeI/BamHI sites to make FRB-Fis1 construct, the insert of which was then PCR amplified and cloned into pBMN-Z vector together with Puro-P2A sequence at HindIII, XhoI and NotI sites by an In-Fusion kit from Clontech to make pBMN-puro-P2A-FRB-Fis1. For receptor translocation assays, wild-type HeLa cells stably expressing FRB-Fis1 were generated using retroviral transduction as described above. Previously generated PINK1Δ110–YFP–2×FKBP (ref. 41) wild-type and kinase-dead and individually each mCherry-tagged autophagy receptor were transfected into FRB-Fis1 stable HeLa cells for 24 h. Cells were then treated with 0.5 μM rapalog (Clontech) for 8 h as previously described[41]. Cells were fixed and stained as described above. Cells were manually counted in a blinded manner for translocation of mCherry-tagged autophagy receptors to mitochondria. Final values represent data collected from 100–150 cells for three independent experiments.

For ULK1 and DFCP1 rescue analysis, pentaKO HeLa cells stably expressing FRB-Fis1 were transiently transfected with PINK1Δ110–YFP–2×FKBP, mCherry–ULK1 and one of the autophagy receptors: Myc–OPTN, Myc–NDP52, Myc–OPTN(F178A), Myc–OPTN(E50K) or Myc–OPTN(Q398X) for 18–24 h. Cells were treated with 0.5 μM rapalog or vehicle for 7 h and imaged live on a Zeiss 780 in a humidified 37 °C, 5% CO_2 chamber. To visualize mitochondria in vehicle-treated controls, cells were pre-incubated for 10 min in 75 nM Mitotracker Deep Red (Invitrogen) before imaging. Fields of PINK1–YFP-positive cells were imaged blindly to the mCherry-containing channel. The images were then blinded and counted manually for translocation of mCherry-tagged ULK1 to mitochondria. Final values represent >75 cells counted over at least two independent experiments.

Mito-Keima mitophagy assay. mt-mKeima[42] (a gift from A. Miyawaki) was cloned into a pCHAC-MCS-1-IRES-MCS2 vector (Allele Biotechnology). PINK1Δ110–YFP–2×FKBP wild-type and kinase-dead were PCR-amplified from the original pC4M-F2E and cloned into pRetroQ-AcGFP-C1 at NheI/XhoI sites by Gibson assembly kit. The HA-tag was removed, and stop codon introduced. Wild-type and pentaKO HeLa cells stably expressing FRB-Fis1, mt-mKeima and either wild-type or kinase-dead PINK1Δ110–YFP–2×FKBP were generated using retroviral transduction as described above. Flag/HA-receptors were stably expressed in these cells by lentivirus transduction as described above then treated with 0.5 μM rapalog for 24 h. Cells were then resuspended in sorting buffer (145 mM NaCl, 5 mM KCl, 1.8 mM $CaCl_2$, 0.8 mM $MgCl_2$, 10 mM HEPES, 10 mM glucose, 0.1% BSA) containing 10 μg ml^{-1} DAPI. Analysis was performed using Summit software (v6.2.6.16198) on a Beckman Coulter MoFlo Astrios cell sorter. Measurements of lysosomal mt-mKeima were made using dual-excitation ratiometric pH measurements at 488 (pH 7) and 561 (pH 4) nm lasers with 620/29 nm and 614/20 nm emission filters, respectively. For each sample, 50,000 events were collected and subsequently gated for YFP/mt-mKeima double-positive cells that were DAPI-negative. Data were analysed using FlowJo (v10, Tree Star).

Statistical calculations. No statistical methods were used to predetermine sample size, and experiments were not randomized. All statistical data were calculated and graphed using GraphPad Prism 6. To assess statistical significance, data from three or more independent experiments were analysed using one-way ANOVA and Tukey's post-test with a confidence interval of 95%. All error bars are expressed as mean ± s.d. In Fig. 4h, i, outliers were removed using ROUT in GraphPad Prism 6 with $Q = 1\%$, and 1–2 values from each condition were removed.

35. Nezich, C. L., Wang, C., Fogel, A. I. & Youle, R. J. MiT/TFE transcription factors are activated during mitophagy downstream of Parkin and Atg5. *J. Cell Biol.* **210,** 435–450 (2015).
36. Santel, A. *et al.* Mitofusin-1 protein is a generally expressed mediator of mitochondrial fusion in mammalian cells. *J. Cell Sci.* **116,** 2763–2774 (2003).
37. Huang, P. *et al.* Heritable gene targeting in zebrafish using customized TALENs. *Nature Biotechnol.* **29,** 699–700 (2011).
38. Hasson, S. A. *et al.* High-content genome-wide RNAi screens identify regulators of parkin upstream of mitophagy. *Nature* **504,** 291–295 (2013).
39. Miller, J. C. *et al.* A TALE nuclease architecture for efficient genome editing. *Nature Biotechnol.* **29,** 143–148 (2011).
40. Mali, P. *et al.* RNA-guided human genome engineering via Cas9. *Science* **339,** 823–826 (2013).
41. Lazarou, M., Jin, S. M., Kane, L. A. & Youle, R. J. Role of PINK1 binding to the TOM complex and alternate intracellular membranes in recruitment and activation of the E3 ligase Parkin. *Dev. Cell* **22,** 320–333 (2012).
42. Katayama, H., Kogure, T., Mizushima, N., Yoshimori, T. & Miyawaki, A. A sensitive and quantitative technique for detecting autophagic events based on lysosomal delivery. *Chem. Biol.* **18,** 1042–1052 (2011).

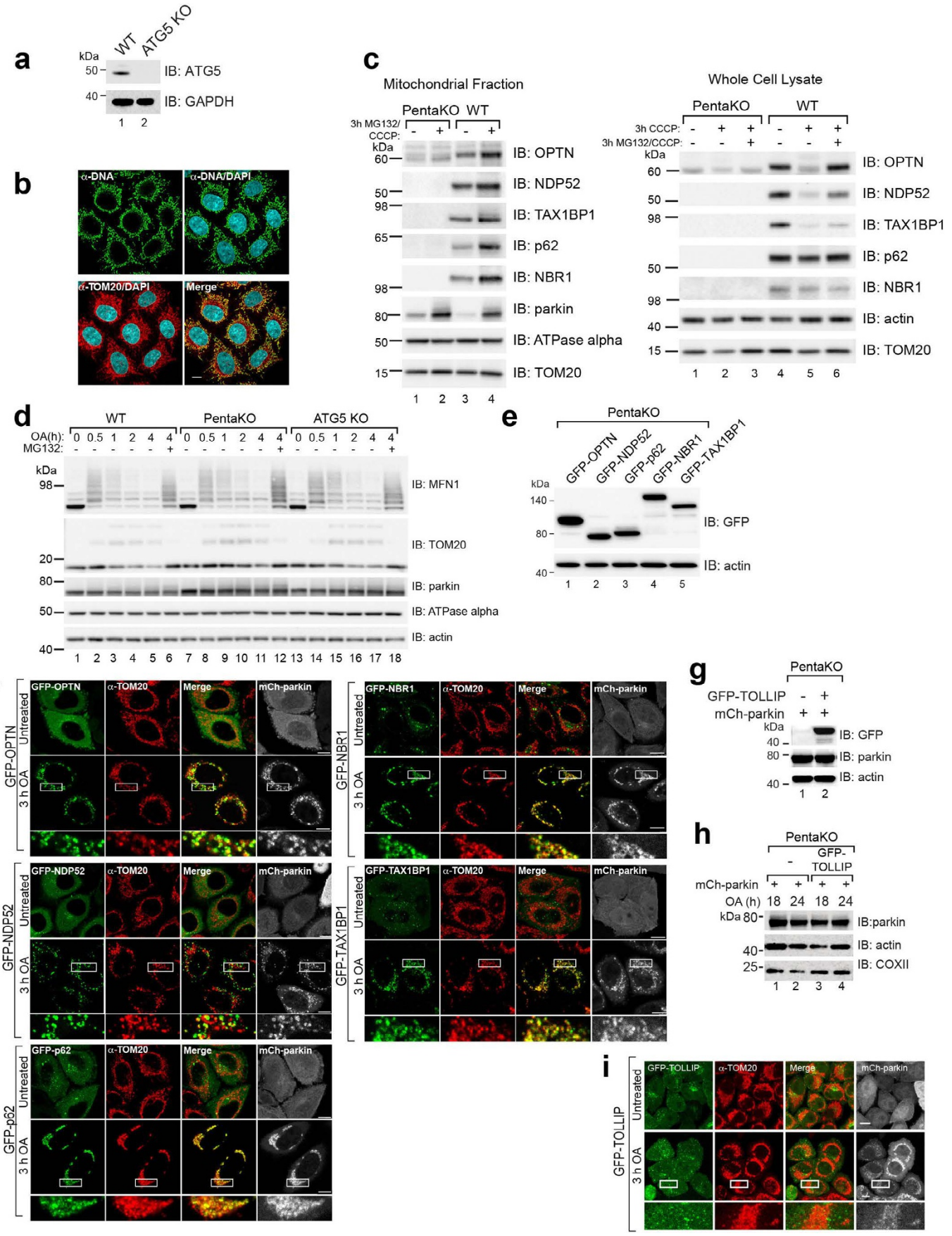

Extended Data Figure 1 | Analysis of knockout cell lines and characterization of autophagy receptor translocation to damaged mitochondria. **a**, The ATG5 knockout cell line was confirmed by immunoblotting. **b**, Representative images of mtDNA nucleoids in HeLa cells immunostained with an anti-DNA antibody (green), confirming colocalization with the mitochondrial marker TOM20 (red) ($n = 3$ experiments). **c**, Mitochondrial fractions from mCherry–parkin expressing pentaKO and wild-type cells were assessed by immunoblotting. **d**, mCh–parkin-expressing wild-type, pentaKO and ATG5 knockouts were treated with oligomycin/antimycin A with or without MG132. Cell lysates were assessed by immunoblotting. **e**, Expression levels of GFP-tagged OPTN, NDP52, p62, NBR1 and TAX1BP1 re-expressed in pentaKO cells by immunoblotting. **f**, Representative images of mCh–parkin-expressing pentaKOs from **e** immunostained for TOM20 ($n = 3$ experiments). **g**, Expression of GFP–TOLLIP in mCh–parkin pentaKOs. **h**, PentaKOs mCh–parkin and with or without GFP–TOLLIP expression were immunoblotted. **i**, Representative images of mCh–parkin pentaKOs expressing GFP–TOLLIP immunostained for TOM20 ($n = 3$ experiments). Scale bars, 10 μm.

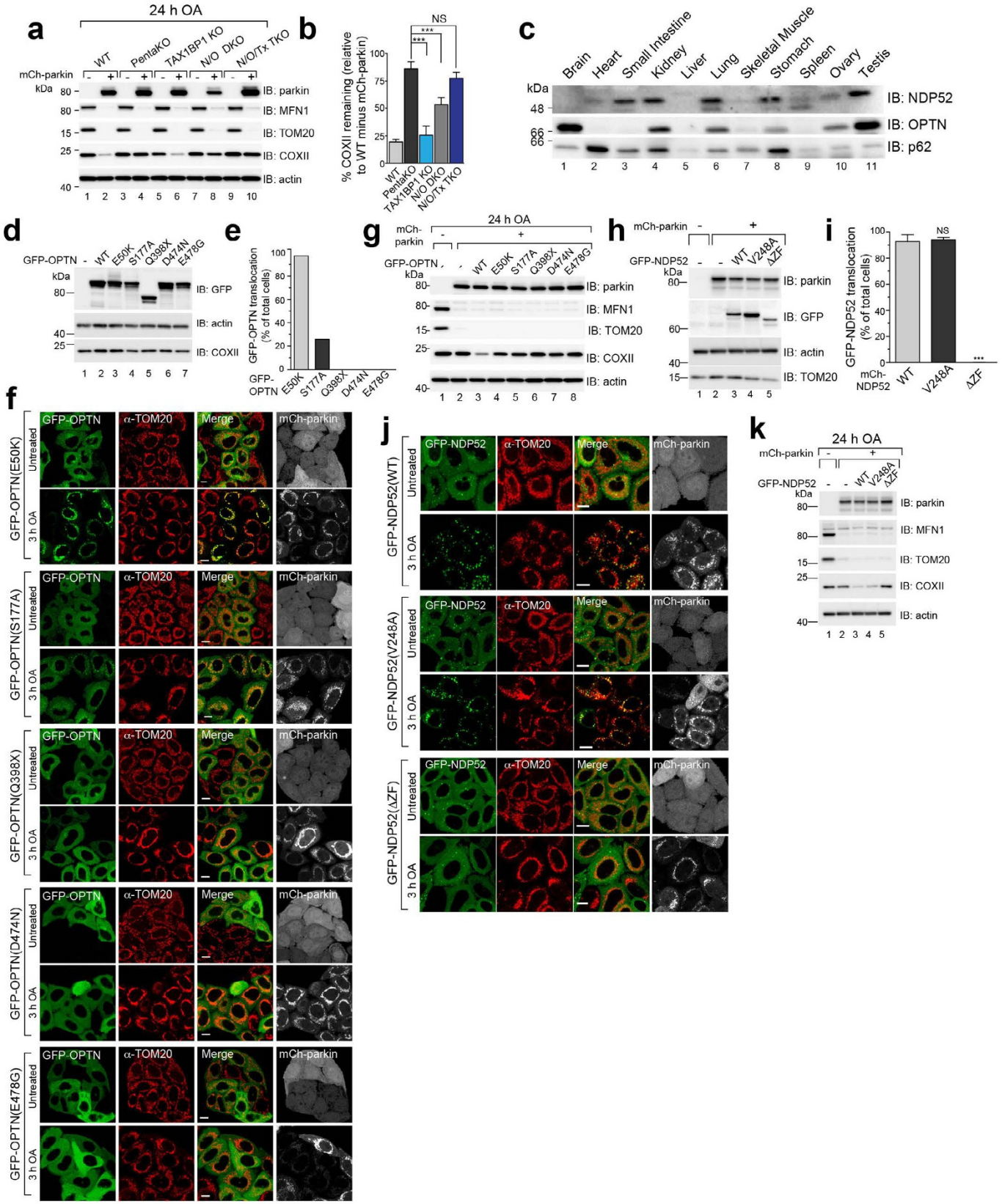

Extended Data Figure 2 | OPTN, NDP52 and TAX1BP1 triple knockout analysis and disease-associated mutations. **a**, **b**, Knockout cell lines with or without mCh–parkin expression were immunoblotted (**a**) and COXII levels were quantified (**b**). **c**, A panel of human tissue lysates was immunoblotted. **d**, Expression of wild-type or mutant GFP–OPTN in mCh–parkin pentaKO cells. **e**, Quantification of cells in **f**. More than 100 cells per condition. **f**, Representative images of mCh–parkin pentaKO cells expressing GFP–OPTN mutants immunostained for TOM20 ($n = 3$). **g**, PentaKOs expressing mCh–parkin were rescued with wild-type or mutant GFP–OPTN, analysed by immunoblotting. See Fig. 2e for quantification of COXII. **h**, Expression of wild-type or mutant GFP–NDP52 in mCh–parkin pentaKO cells. **i**, Quantification of cells in **j**. More than 100 cells per condition. **j**, Representative images of mCh–parkin pentaKOs expressing wild-type or mutant GFP–NDP52 were immunostained for TOM20 ($n = 3$). **k**, PentaKO cells expressing mCh–parkin rescued with wild-type or mutant GFP–NDP52 were analysed by immunoblotting. See Fig. 2f for quantification of COXII. Data are mean ± s.d. from three (**b** and **i**) and two (**e**) independent experiments. ***$P < 0.001$ (one-way ANOVA). Scale bars, 10 μm.

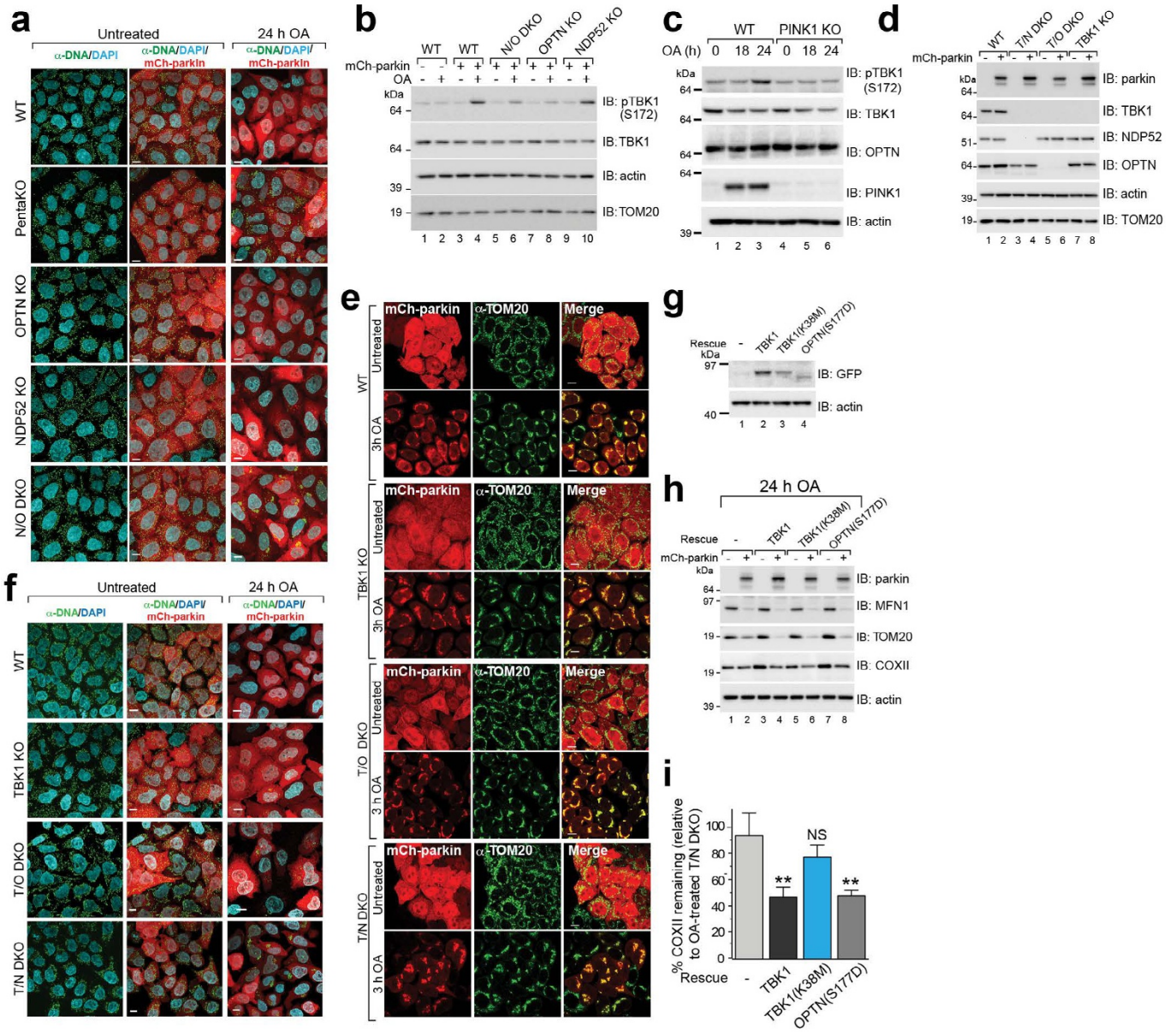

Extended Data Figure 3 | TBK1 activates OPTN in PINK1/parkin mitophagy. **a**, Representative images of untreated mCh–parkin cells and merged images of treated cells as indicated immunostained for DNA. See Fig. 2a for anti-DNA and DAPI images of treated samples ($n = 3$). **b**, Cell lysates from wild-type, NDP52/OPTN DKO, OPTN knockout and NDP52 knockout cells with or without mCh–parkin expression were immunoblotted for TBK1 activation. **c**, Cell lysates from wild-type and PINK1 knockout cells without parkin expression were immunoblotted for TBK1 activation (S172 phosphorylation). **d**, Confirmation of TBK1/NDP52 DKO, TBK1/OPTN DKO and TBK1 knockout by immunoblotting. **e**, Knockout cell lines from **d** were immunostained for TOM20 ($n = 3$). **f**, Representative images of untreated mCh–parkin wild-type and knockout cells, and merged images of treated cells as indicated were immunostained for DNA. See Fig. 2g for anti-DNA/DAPI images treated samples ($n = 3$). **g**, TBK1/NDP52 DKO cells rescued with GFP–TBK1 wild-type or K38M, or GFP–OPTN(S177D) and were assessed by immunoblotting. **h**, Cells in **g** were assessed by immunoblotting. **i**, Quantification of COXII levels in **h** displayed as mean ± s.d. from three independent experiments. $^{**}P < 0.005$ (one-way ANOVA). Scale bars, 10 μm.

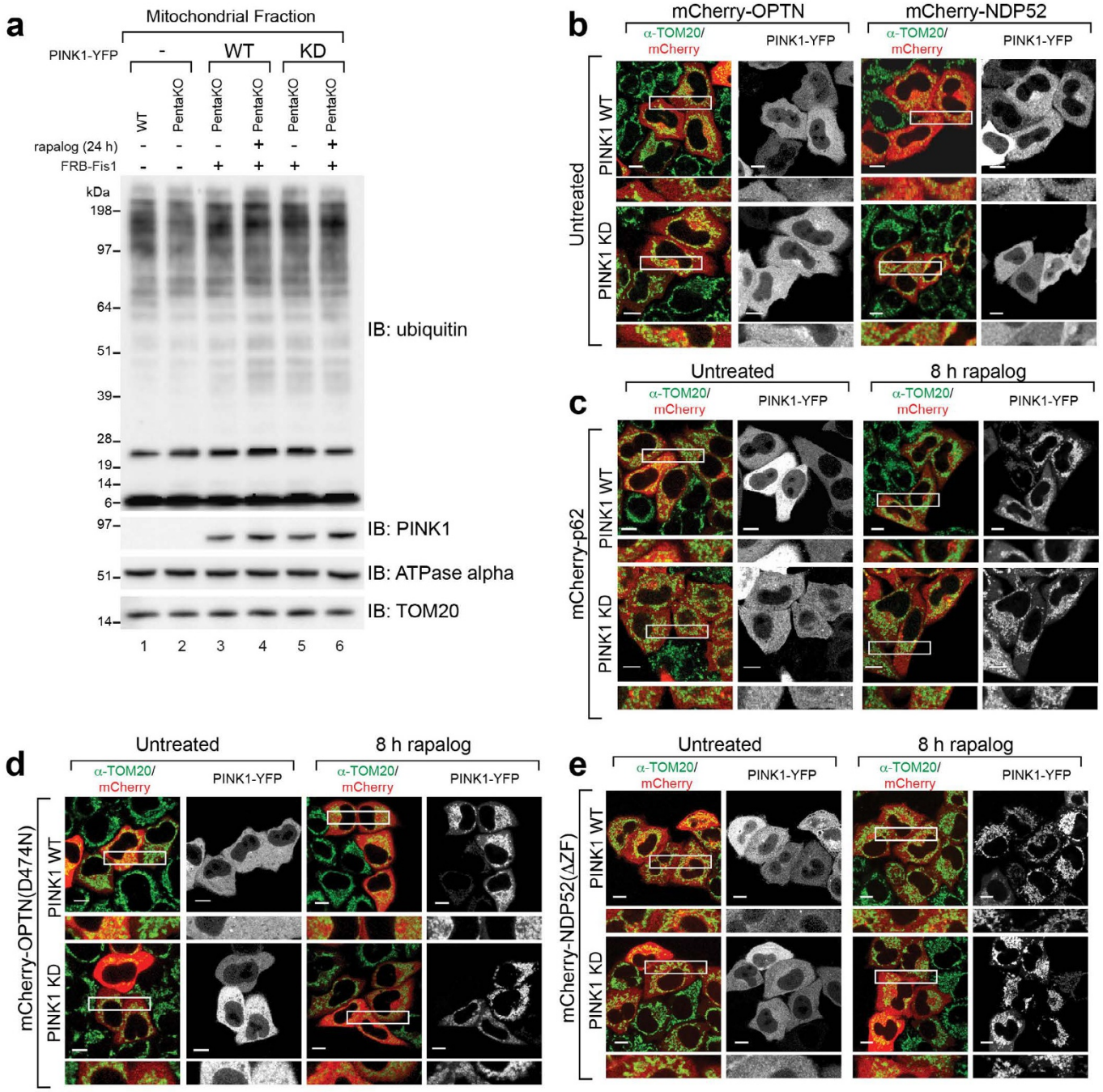

Extended Data Figure 4 | Parkin-independent recruitment of receptors to mitochondria through PINK1 activity. **a**, Isolated mitochondria from wild-type and pentaKO cells with or without FRB-Fis1 and with wild-type or kinase-dead PINK1Δ110–YFP–2×FKBP were immunoblotted. **b**–**e**, Representative images of pentaKO cells expressing FRB-Fis1, wild-type or kinase-dead PINK1Δ110–YFP–2×FKBP, and mCh–OPTN or mCh–NDP52 (**b**), mCh–p62 (**c**), mCh–OPTN(D474N) (**d**) or mCh–NDP52(ΔZF) (**e**). Cells were untreated (**b**) or treated with rapalog (**c**–**e**) and immunostained for TOM20. All images are representative of three independent experiments. See Fig. 3b for quantification. Scale bars, 10 μm.

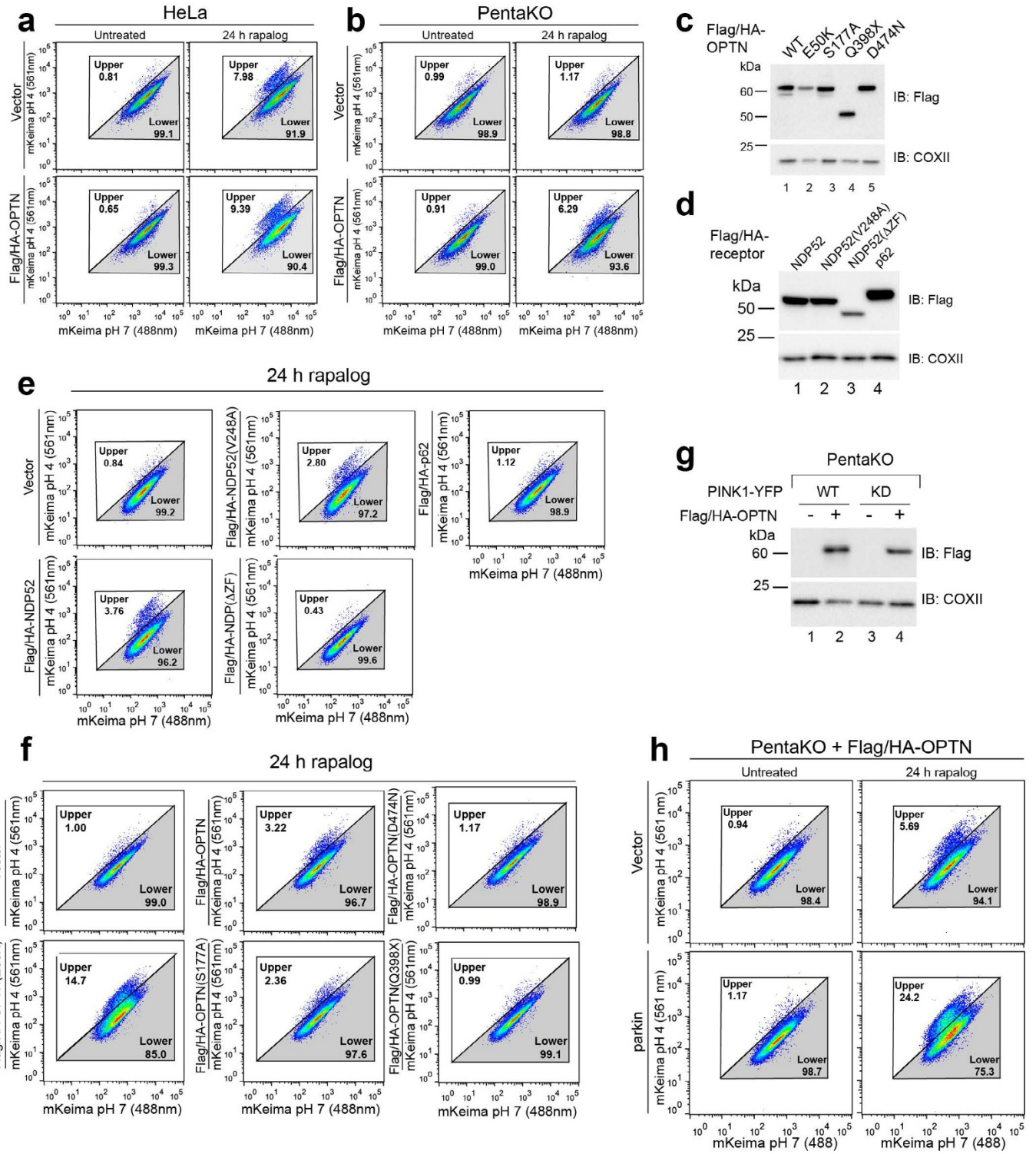

Extended Data Figure 5 | PINK1 directly stimulates mitophagy in the absence of mitochondrial damage. **a**, **b**, Cells were treated with rapalog and analysed by FACS for lysosomal-positive mt-mKeima. Representative data for wild-type HeLa (**a**) and pentaKO cells (**b**) without or with Flag/HA–OPTN. **c**, **d**, Cell lysates from pentaKO cells expressing FRB-Fis1, PINK1Δ110–YFP–2×FKBP, mt-mKeima and wild-type Flag/HA–OPTN (**c**) or mutants, (**d**) Flag/HA–p62, wild-type Flag/HA–NDP52 or NDP52 mutants as indicated were assessed for receptor expression by immunoblotting. **e**, **f**, Cells from **c** and **d** were treated with rapalog and analysed by FACS for lysosomal-positive mt-mKeima. Representative data of two experiments are presented. **g**, Cell lysates from pentaKO cells expressing FRB-Fis1, with or without Flag/HA–OPTN and wild-type or kinase-dead PINK1Δ110–YFP–2×FKBP were assessed for OPTN by immunoblotting. **h**, Flag/HA–OPTN pentaKO cells expressing FRB-Fis1, PINK1Δ110–YFP–2×FKBP, mt-mKeima-transfected and either vector or untagged parkin were analysed by FACS. Representative data of two experiments are presented.

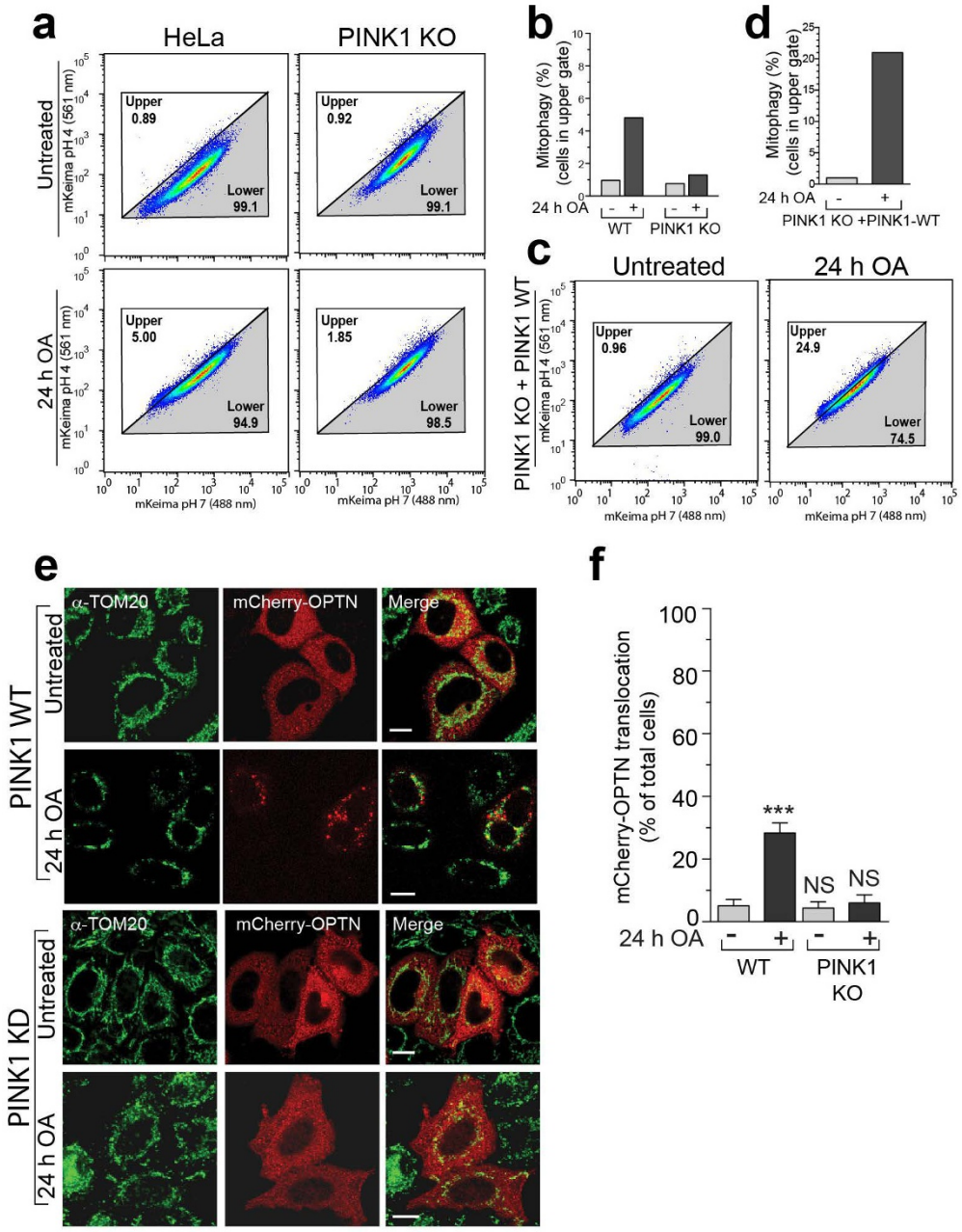

Extended Data Figure 6 | PINK1 directly stimulates mitophagy after mitochondrial damage. **a**, **c**, Representative FACS data of mt-mKeima-expressing wild-type or PINK1 knockout HeLa cells (**a**) or PINK1 knockout cells rescued with PINK1 wild-type and then untreated or treated with oligomycin and antimycin A (**c**). **b**, **d**, Average percentage of mitophagy for two replicates of **a** and **c**, respectively. **e**, Representative images of wild-type HeLa cells expressing mCh–OPTN and treated with oligomycin and antimycin A as indicated and immunostained for TOM20 ($n = 3$). **f**, Quantification of mCh–OPTN translocation from cells in **e**. Data are mean ± s.d. from three independent experiments. $^{***}P < 0.001$ (one-way ANOVA). NS, not significant.

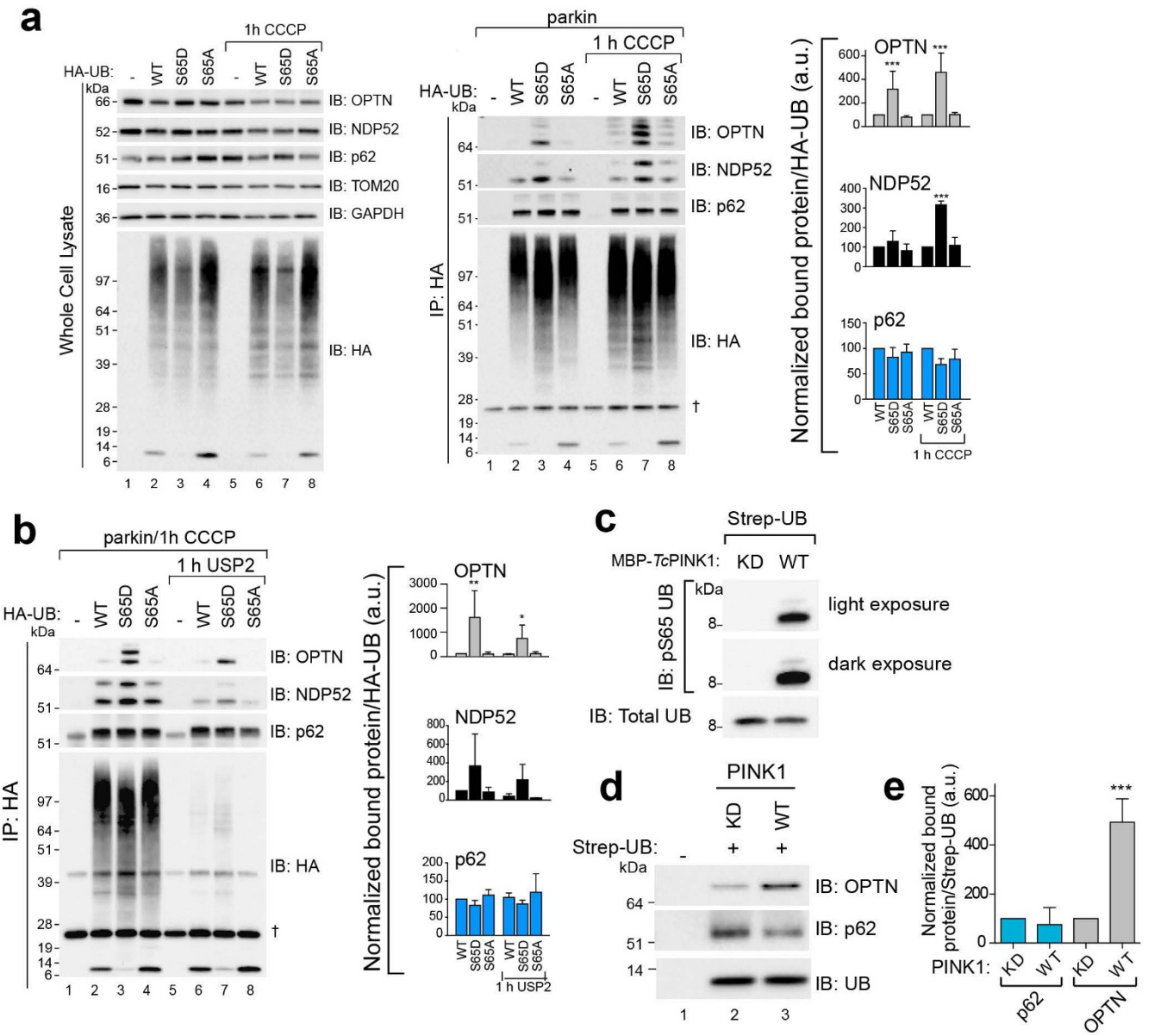

Extended Data Figure 7 | OPTN and NDP52 preferentially bind phosphomimetic ubiquitin. **a**, HeLa cells expressing mCh–parkin and wild-type HA–ubiquitin (HA–UB) or mutants S65D or S65A were treated with CCCP. HA–ubiquitin was co-immunoprecipitated and the bound fraction was analysed by immunoblotting. Quantifications of the total bound fraction of OPTN, NDP52 and p62 are shown. **b**, HA–ubiquitin transfected into HeLa cells with mCh–parkin were then treated with CCCP, and HA–ubiquitin was immunoprecipitated. The bound fraction was treated with the deubiquitinase USP2, and washed to remove all unbound protein after deubiquitination. Quantification of the total bound fraction of OPTN, NDP52 and p62 are shown on the right. **c**, **d**, Strep-tactin-tagged ubiquitin (strep–UB) was incubated with either wild-type or kinase-dead PINK1 in an *in vitro* phosphorylation reaction, immunoblotted with an anti-phosphoS65 ubiquitin antibody (**c**), and then incubated with cytosol collected from untreated, wild-type HeLa cells. The ubiquitin was then pulled down using strep-tactin beads and analysed by immunoblotting (**d**). **e**, Quantification of bound OPTN and p62 normalized to total ubiquitin. Data in **a**, **b** and **e** are mean ± s.d. from three independent experiments. $*P < 0.05$, $**P < 0.005$, $***P < 0.001$ (one-way ANOVA). Dagger symbol denotes nonspecific band.

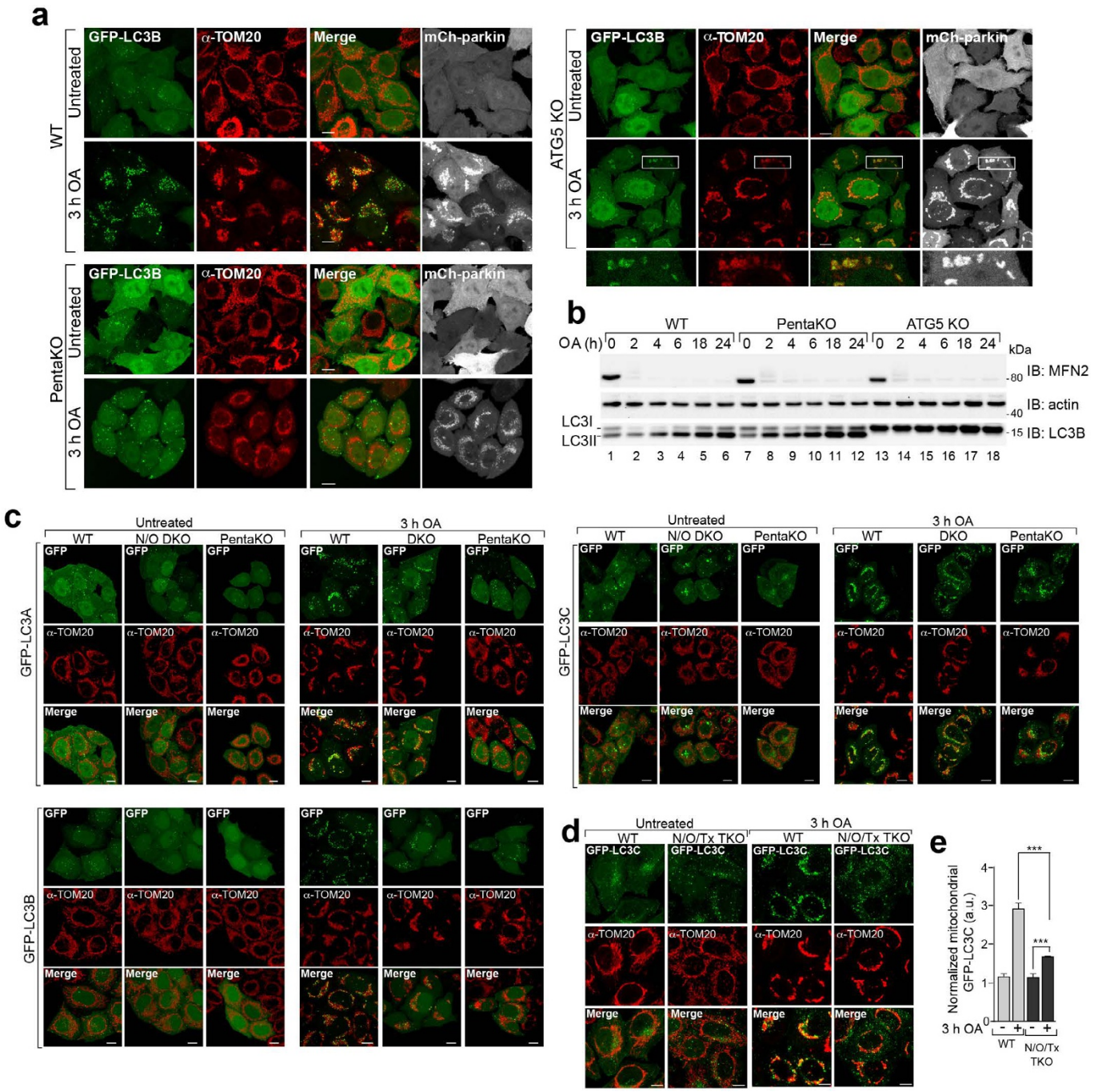

Extended Data Figure 8 | Analysis of LC3 family members and their translocation to damaged mitochondria in autophagy receptor knockout cell lines. a, Representative images of wild-type, pentaKO and ATG5 knockout HeLa cells expressing mCh–parkin and GFP–LC3B were immunostained for TOM20 ($n = 3$). **b**, Cell lysates from mCh–parkin expressing wild-type, pentaKO and ATG5 knockout cells were immunoblotted. **c**, Representative images of wild-type, NDP52/OPTN DKO and pentaKO cells expressing mCh–parkin and GFP-tagged LC3A, LC3B or LC3C were immunostained for TOM20 ($n = 3$; see Fig. 4a for quantification). **d**, **e**, Representative images of wild-type and NDP52/OPTN/TAX1BP1 triple knockout cells expressing mCh–parkin and GFP–LC3C were immunostained for TOM20 ($n = 3$) (**d**) and quantified for GFP–LC3C translocation to mitochondria (**e**). Data in **e** are mean ± s.d. from three independent experiments. $^{***}P < 0.001$ (one-way ANOVA). Scale bars, 10 μm.

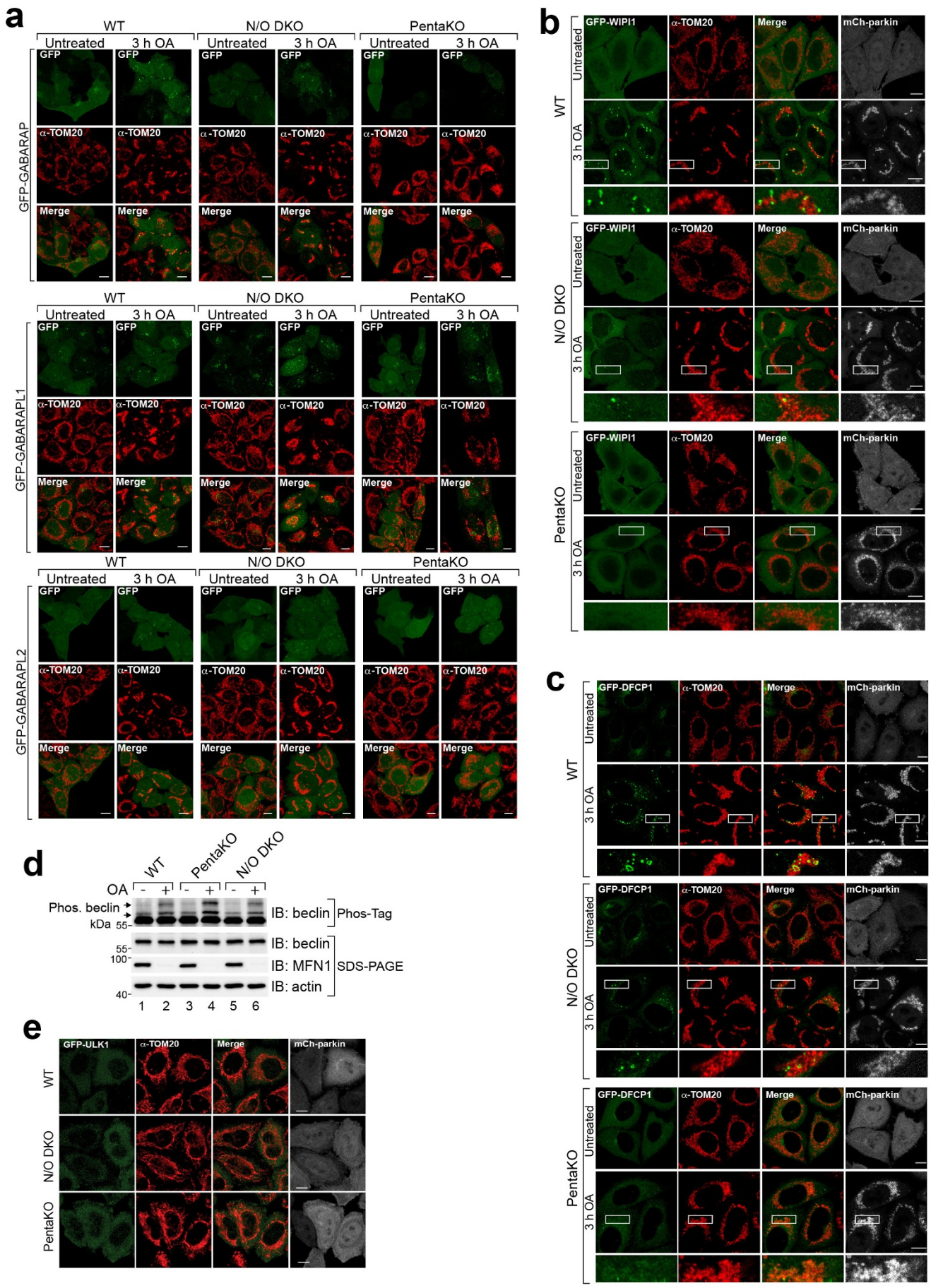

Extended Data Figure 9 | GABARAP proteins do not translocate to damaged mitochondria, and early stages of autophagosome biogenesis mediated by WIPI1 and DFCP1 are inhibited in autophagy-receptor-deficient cell lines. **a**–**c**, Representative images of wild-type, NDP52/OPTN DKO and pentaKO cells expressing mCh–parkin and GFP-tagged GABARAP, GABARAPL1 or GABARAPL2 (**a**), GFP–WIPI1 (**b**) or GFP–DFCP1 (**c**) immunostained for TOM20 ($n = 3$ for each condition, see Fig. 4b and c for quantification of **b** and **c**). **d**, mCh–parkin cell lines as indicated were subjected to either phos-tag SDS–PAGE or standard SDS–PAGE followed by immunoblotting. Arrows indicate the position of phosphorylated beclin species. **e**, Representative images of untreated wild-type, NDP52/OPTN DKO and pentaKO cell lines expressing mCh–parkin and GFP–ULK1 were immunostained for TOM20 and GFP ($n = 3$ experiments). Scale bars, 10 μm.

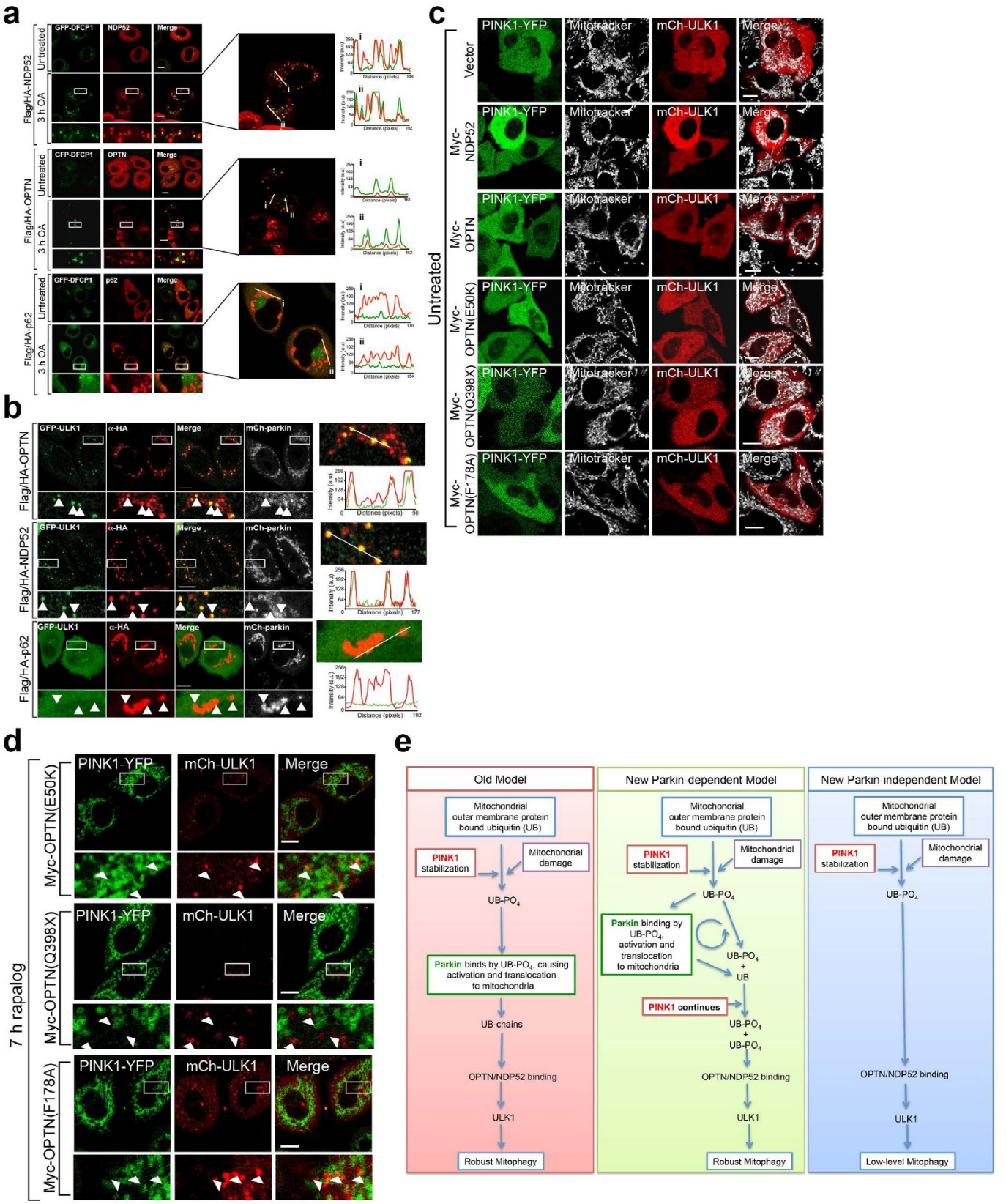

Extended Data Figure 10 | OPTN and NDP52 rescue DFCP1 and ULK1 recruitment deficit in pentaKOs. **a**, Representative images of pentaKO cells expressing mCh–parkin, GFP–DFCP1 and the indicated Flag/HA-tagged autophagy receptors immunostained for haemagglutinin ($n = 2$ experiments). Panels on the right display co-localization of Flag/HA-tagged constructs and GFP–DFCP1 by fluorescence intensity line measurement. **b**, Representative images of pentaKO cells expressing mCh–parkin and GFP–ULK1 that were rescued by Flag/HA–OPTN, Flag/HA–NDP52 and Flag/HA–p62, and immunostained for haemagglutinin and GFP. Arrows indicate HA-tagged receptor puncta ($n = 2$). Right panels display colocalization of haemagglutinin and GFP by fluorescence intensity line measurement. **c**, **d**, Representative images of pentaKO cells stably expressing FRB-Fis1 and transiently expressing PINK1Δ110–YFP–2×FKBP and vector or Myc-tagged receptors, that were untreated (**c**) or treated with rapalog (**d**) and imaged live ($n = 3$ experiments, see Fig. 4h, i for quantification of **c**, **d**). Scale bars, 10 μm. **e**, Old and new models of PINK1/parkin mitophagy. The old model is dominated by parkin ubiquitination of mitochondrial proteins. In this, PINK1 has a small initiator role with the main function being to bring parkin to the mitochondria. The new model depicts parkin-dependent and -independent pathways leading to robust and low-level mitophagy, respectively. On the basis of our data, PINK1 is central to mitophagy both before and after parkin recruitment by phosphorylating ubiquitin to recruit parkin and autophagy receptors to mitochondria, to induce clearance. In the absence of parkin (right), this occurs at a low level owing to the relatively low basal ubiquitin levels on mitochondria. When parkin is present, it serves to amplify the PINK1 generated phospho-ubiquitin signal, allowing for robust and rapid mitophagy induction.